ABSTRACT

Title of Thesis:	APPLICATIONS OF MACROCYCLIC LIGANDS IN C-H ACTIVATION AND OLEFIN AZIRIDINATION REACTIONS
	Fan Yang, Master of Science, 2017
Thesis directed by:	Prof. Andrei N. Vedernikov Department of Chemistry & Biochemistry

The cyclic tridentate ligand [2.1.1]-(2,6)-9,16-dioxapyridinophane (O_2-L), in analogy to the previously reported macrocycle [2.1.1]-(2,6)-pyridinophane (L), has been prepared for potential applications in C-H activation/functionalization. Studies of the d^8 complex (O_2-L)$PdCl_2$ reveals that only two of the three nitrogen atoms in O_2-L bind to the metal; the Pd atom migrates quickly between the two nitrogen atoms tethered by the ethylene linkage at room temperature. The complex (O_2-L)Cu^+ exhibited outstanding performance in promoting direct aziridination reactions, furnishing aziridines from olefins and PhINTs in near-quantitative yields in the absence of bulky substituents attached to the olefin C=C bonds. The complex $[LPt^{IV}H_2Me]^+$ was found to cleave CH bonds of disubstituted benzenes with exceptional regioselectivity, as a result of the reaction's sensitivity to sterics. Mechanistic studies suggest that the dissociation of an alkane or arene molecule from the Pt^{II}-alkane/arene σ-complex requires high activation energy and is rate-limiting.

APPLICATIONS OF MACROCYCLIC LIGANDS IN C-H ACTIVATION AND OLEFIN AZIRIDINATION REACTIONS

by

Fan Yang

Thesis submitted to the Faculty of the Graduate School of the
University of Maryland, College Park, in partial fulfillment
of the requirements for the degree of
Master of Science
2017

Advisory Committee:
Prof. Andrei N. Vedernikov, Chair
Prof. Philip DeShong
Prof. Bryan Eichhorn
Prof. Osvaldo Gutierrez

Acknowledgements

My sincere thanks go to my mentor, Professor Andrei Vedernikov. During my two years of research in his lab, he provided me with invaluable advice and guidance. As a mentor he has allowed me to pursue novel research ideas and encouraged me to persevere when my experiments didn't work. He was always supportive and kind.

Throughout the two years I had the pleasure of working along with Elikplim Abada, David Watts, Daniel Adams, Courtney Love, Vincent Wu and Jiaheng Ruan. I'm very grateful for their advice and friendship. Special thanks to my desk and bench neighbor David Watts. He provided a lot of help on my research and was always patient to talk about the chemistry with me when I encountered problems.

I want to extend my thanks to Dr. Philip DeShong, Dr. Bryan Eichhorn and Dr. Osvaldo Gutierrez, for agreeing to serve on my thesis committee and reserving time for it.

Our department enjoys the services of the NMR staff Dr. Yiu-Fai Lam, Dr. Fu Chen and Dr. Yinde Wang, the X-ray crystallographer Dr. Peter Zavalij and the mass spectropist Dr. Yue Li. I have been assisted by them on many occasions and I appreciate their competence and enthusiasm.

Table of Contents

Acknowledgements ii

List of Schemes iv

List of Figures v

Chapter 1: Introduction and background 1

1.1 Pt(II) Mediated C-H Activation 1

1.2 Transition Metal Catalyzed Direct olefin Aziridination 5

Chapter 2: Results and Discussions 8

2.1 Synthesis of [2.1.1]-(2,6)-9,16-dioxapyridinophane (O_2-L) 8

2.2 Coordination of O_2-L with Transition Metals 9

2.3 Direct Olefin Aziridination Catalyzed by (O_2-L)Cu^+ 13

2.4 C-H Activation with $[LPtH_2Me]^+$ 16

2.5 Conclusions and Future Work 22

Supplemental Materials 24

General Information 24

Synthesis 25

Spectra 31

References 40

List of Schemes

Scheme 1: Currently accepted mechanism of the Shilov cycle ····· 1

Scheme 2: Mechanisms for ligand substitution at Pt(II) ····· 2

Scheme 3: Direct and dissociative mechanisms for alkane elimination at Pt(IV) ····· 3

Scheme 4: General synthetic pathways affording aziridines ····· 6

Scheme 5: The preparation of [2.1.1]-(2,6)-9,16-dioxapyridinophane (O_2-L) ····· 8

Scheme 6: Substrate scope for direct olefin aziridination catalyzed by (O_2-L)Cu^+ ····· 14

Scheme 7: The preparation of $[LPtH_2Me]^+$ and its X-ray diffraction structure ····· 17

List of Figures

Figure 1: Qualitative relation between the degree of out-of-plane deformation of d^8 coordination units and the thermodynamics of methane addition. 2

Figure 2: (a) Ligand L and Me_4-L; (b) DFT-optimized structure of $[LPtMe]^+$. 4

Figure 3: (a) The preparation of $(O_2$-L)$PdCl_2$ and its X-ray diffraction structure; (b) ^{1}H NMR spectra of $(O_2$-L)$PdCl_2$ at 22 °C and -40 °C 10

Figure 4: Symmetric and unsymmetric isomers of $(O_2$-L)$PdCl_2$ 11

Figure 5: ^{1}H NMR spectrum of $(O_2$-L)CuCl. 12

Figure 6: Selected reported transition metal catalysts for direct olefin aziridination. 16

Figure 7: DFT-calculated Gibbs free energy of methane elimination versus H_2 elimination from $[LPtMeH_2]^+$ 18

Figure 8: (a) The reaction of $[LPtH_2Me]^+$ with arenes to afford $[LPtH_2Ar]^+$; (b) Comparison of the hydride signals of $[LPtH_2Ph]^+$ and $[LPtH_2Me]^+$ 19

Figure 9: The reaction of $[LPtMeH_2]^+$ with PhH/m-$C_6H_4F_2$ mixture affords the two products in a constant ratio of 1:2.48 21

Figure 10: Calculated Gibbs free energies for the conversion of $[LPtMeH_2]^+$ to $[LPtArH_2]^+$. 22

Chapter 1: Introduction and background

1.1 Pt(II) Mediated C-H Activation

H/D exchange of arenes catalyzed by Pt(II) in aqueous acetic acid, first reported by Garnett and Hodges in 1967[1], was the earliest documented example of intermolecular C−H activation by a transition-metal complex. Two years later in 1969, Shilov extended the work to C−H functionalization of methane by adding $[PtCl_6]^{2-}$ as an oxidant to the system[2] (Scheme 1). The new combination was able to oxidize methane to a mixture of methanol and methyl chlorides at temperatures around 120 °C.

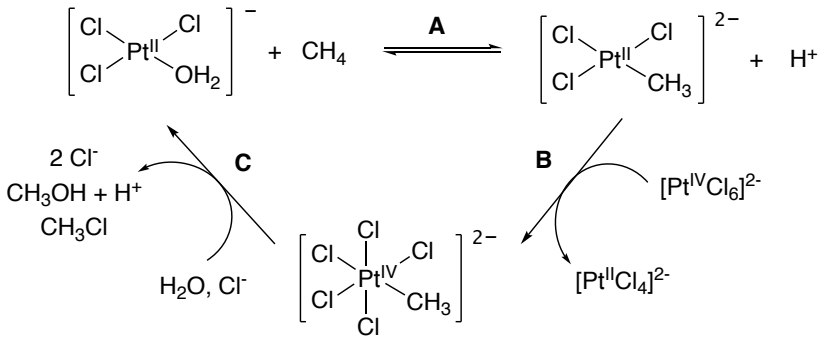

Scheme 1: Currently accepted mechanism of the Shilov cycle. The first step (A) is the C-H activation of CH_4 to make an H_3C-Pt(II) intermediate which is subsequently (B) oxidized by $[PtCl_6]^{2-}$. The final step (C) includes reductive elimination of methanol or methyl chloride via nucleophilic attack by water or Cl^-.

Since the discovery of Shilov system, C-H activation by Pt has been mostly studied at square-planar Pt(II) complexes[3,4]. Mechanistically, all C-H activation reactions at Pt(II) are believed to proceed by the same initial step (Scheme 2): the substitution of one of the ligands by a hydrocarbon substrate, to form a σ-alkane or arene complex prior to the reversible C-H bond cleavage[3]. The substitution may occur dissociatively via a three-coordinate, 14-electron intermediate, or associatively via a five-coordinate, 18-electron intermediate, or by a concerted interchange mechanism via a five-coordinate transition state[5,6]. It has been established that the majority of substitution reactions at Pt(II) occur associatively[7,8], while the dissociative process commonly involves relatively electron-rich

complexes with a strong σ donor trans to the leaving group[9], as in the example of $[PtCl_4]^{2-}$.

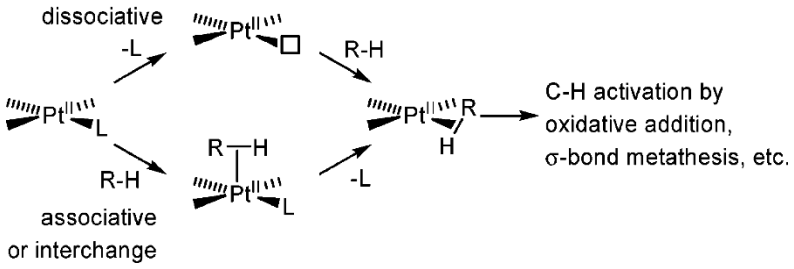

Scheme 2: Different mechanisms for ligand substitution by hydrocarbon molecules at Pt(II)

Studies have shown that the displacement of a ligand by a hydrocarbon substrate at Pt(II) to form a Pt(II)-hydrocarbon complex always constitutes a significant part of the overall barrier for C-H activation[3]. In fact, this step is often believed to be rate-limiting. Once the σ or π complex has been formed, C-H bond cleavage is quite facile, as evidenced by the numerous instances of H/D scrambling reactions.

The ability of Pt(II) to coordinate with a hydrocarbon substrate and subsequently split the CH bonds is strongly dependent on the ligand environment L. In particular, the degree of out-of-plane deformation of the ligands from the square planar geometry preferred by Pt(II) plays a critical role in controlling the reactivity of the Pt(II) species[9]. Multidentate ligands that cannot accommodate coplanar coordination with the metal due to structural restraints

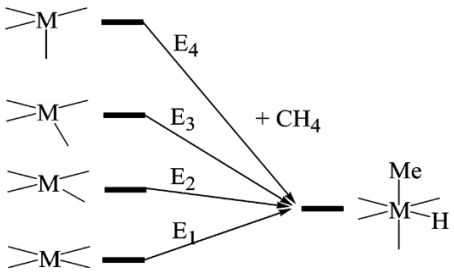

Figure 1: Qualitative relation between the degree of out-of-plane deformation of a d^8 precursor coordination unit and the thermodynamics of methane addition.

allows only intermediate stabilization of the complexes, and thus benefit the formation of

metal-hydrocarbon σ-complexes, both thermodynamically and kinetically, as summarized in Figure 1.

Pt(IV) alkyl hydrides of intermediate thermodynamic and kinetic stability that are derived from destabilized Pt(II) complexes are also of high interest because they can easily eliminate alkanes and furnish the corresponding reactive Pt(II) complexes[3,4,10,11]. Reductive elimination of C-X (X = H, C, Cl, etc.) at Pt(IV) usually proceeds either dissociatively, via a 16-electron, five-coordinate intermediate, or by direct reductive elimination mechanism, as illustrated in Scheme 3. It has been suggested that dissociative behavior may be expected for monodentate ligands while direct elimination is preferred by chelating ligands because of their stronger binding with the metals[3]. We infer that bidentate/tridentate ligands that form constrained octahedral complexes with the d^6 metals may lower the energy barrier associated with the dissociative pathway, by retracting one donor atom from the metal-ligand coordination easily, and thus give rise to fast C-X elimination from the metal under mild conditions.

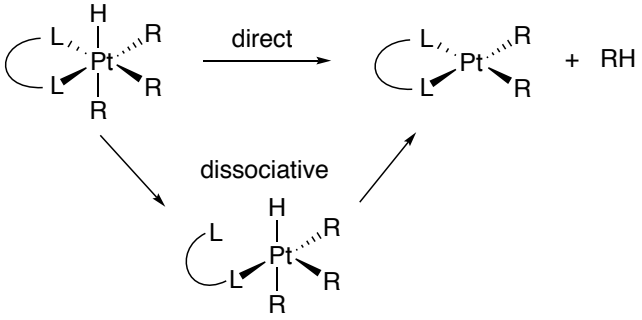

Scheme 3: Direct and dissociative mechanisms for alkane elimination from Pt^{IV}. R is an alkyl group.

Vedernikov has published work that evidences the above ligand design idea[9-13]. The novel cyclic tridentate ligand **L** synthesized by him and co-workers, as shown in Figure 2a, possesses a rigid structure. The three nitrogen donor atoms in L cannot be arranged in one

plane with the Pt–C bond due to the structure constraints, thus the formation of a stable (i.e., less reactive) 16-electron square planar complex is prevented. The T-shaped, 14-electron $[LPt^{II}R]^+$ (R = H or Me; Fig. 2b) transient species binds with hydrocarbons R′H and cleaves the CH bonds easily[10,12]. The resulting octahedral products $[LPt^{IV}RR'(H)]^+$ are also only modestly stabilized, so that the $[LPt^{II}(R, R')]^+$ precursors can be readily accessible from these Pt^{IV} species and be involved in facile β-hydride elimination (R or R′ = alkyl with β-CH bonds). For R = H a reversible alkane R′H addition to Pt(II) center can be observed at relatively low (80 – 90 ^{o}C) temperatures.

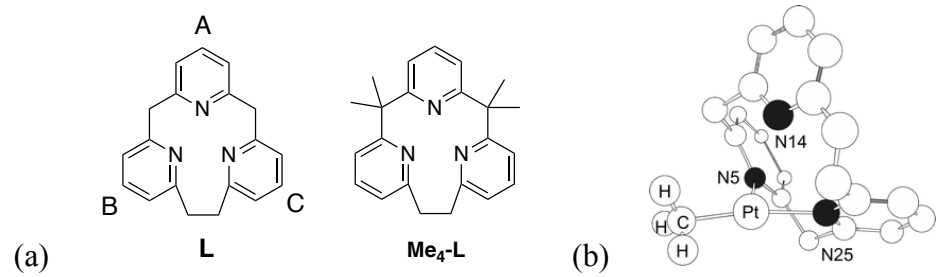

Figure 2: (a) The structures of ligand L and Me_4-L; (b) DFT-optimized structure of $[LPtMe]^+$ cation. Selected bond lengths and angles: Pt–N(5), 1.993 Å; Pt–N(14), 3.026 Å; Pt–N(25), 2.171 Å; Pt–C(41), 2.042 Å; N(5)–Pt–N(25), 85.3; N(5)–Pt-C(41), 100.5; N(25)–Pt–C(41), 171.3.

A major concern about the transient complex $[LPt^{II}R]^+$ is that the bridging methylene groups of the ligand are in close proximity to the Pt center. This proximity may cause undesired transformations involving the methylene CH bonds, which is presumably associated with the decomposition of such complexes, especially under oxidizing conditions. The analogue Me_4-L has the potential to avoid the undesired CH activation. However, Me_4-L is more difficult to bind to a metal because of the significant hindrance imposed by the four methyl groups.

This work aims to extend the study of the $[LPt^{II}H]^+$ complex and explore its applications

in CH activation reactions. In addition, much effort is put on the synthesis of new analogues of L where the CH_2 linkers are replaced with O atoms, which are expected to be more robust toward oxidative degradation. Result of such attempts are described in Chapter 2.

1.2 Transition Metal Catalyzed Direct olefin Aziridination

Aziridines are among the most useful heterocyclic intermediates in organic synthesis, acting as precursors of many complex molecules including biologically active compounds due to the strain incorporated in their skeletons[14,15]. The high strain energy associated with the aziridine ring enables easy cleavage of the CN bond. Therefore, aziridines can either undergo ring cleavage reactions with a range of nucleophiles through a stereo-controlled manner or cycloaddition reactions with dipolarophiles, providing access to a wide range of important nitrogen-containing products[15-18].

In view of their interesting chemical peculiarities and the scarcity of widespread procedures for their preparation, the scientific community is constantly interested in the development of new synthetic protocols which are more efficient than traditional methods such as cyclization of amino alcohols, the reaction between imines and carbene precursors, e.g., diazo-containing compounds, or nitrene transfer to C=C bond (Scheme 4)[18-21]. Among the available synthetic strategies, direct aziridination of alkenes promoted by transition metal complexes is a very interesting and promising approach, due to the affordability and easy accessibility of the olefin substrates.

Iminoiodinane compounds[22], haloamine-T salts[23] and organic azides[24,25] represent the most applied classes of nitrogen sources in direct olefin aziridination reactions. On the

other hand, numerous transition metal catalysts have demonstrated to be efficient promoters of nitrene transfer reactions[22,26-27].

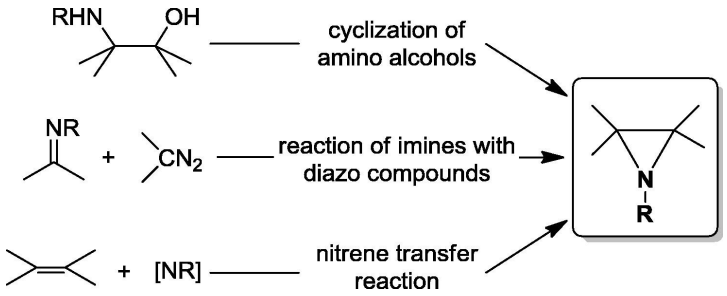

Scheme 4: General synthetic pathways affording aziridines.

In 2003 Vedernikov, *et al.* reported the synthesis of the complex $[LCu^{I}]^{+}$ and explored its catalytic activity in direct olefin aziridination reactions using PhINTs as the nitrene source[28]. It was found that the complex allows very fast (2-10 min at 0-20 °C) and often high-yield conversion of simple mono-, di-, tri-, and tetra- substituted olefins including those with electron-withdrawing groups attached to the C=C bond (eq. 1). The high catalytic performance of the complex in the aziridination reactions is proposed to originate largely from the rigid structure of ligand L and the use of weakly coordinating solvents (CH_2Cl_2, $CHCl_3$) and counterions (BAr^{F}_4). The constrained structure of L is poorly suited for the near-tetrahedral or trigonal planar geometries preferred by Cu(I), thus helps in producing $LCu^{III}(NTs)^{+}$ (eq. 2), a plausible key intermediate in the catalytic cycle of the direct aziridination reaction.

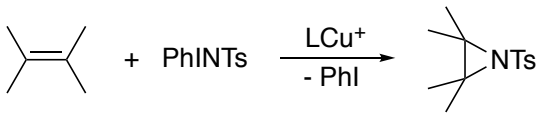

(1)

$$PhINTs + [(\eta^3\text{-}L)Cu^{I}]^{+} \longrightarrow PhI + [LCu^{III}(NTs)]^{+} \qquad (2)$$

As mentioned in section 1.1, we have spent efforts on the preparation of new ligands that

are structurally similar to L. We expect the new ligands, possessing similar rigid structures with L but holding different electronic properties, to find application not only in CH activations, but also in direct olefin aziridination reactions. Results of the exploration shall be forthcoming in next chapter.

Chapter 2: Results and Discussions

2.1 Synthesis of [2.1.1]-(2,6)-9,16-dioxapyridinophane (O_2-L)

In order to avoid undesired CH activation at the bridging methylene groups of ligand L and to prevent the associated decomposition of $[LM]^{n+}$, we proposed to replace the methylene groups of L with heteroatoms. Oxygen is a good choice because of its similar size with carbon. The corresponding analogue O_2-L is presumed to own a constrained structure similar to L, while the electron-withdrawing inductive effect imposed by the two oxygen atoms will slightly decrease the electron donating ability of the nitrogen lone pairs residing in non-bonding sp^2 orbitals. This change in ligand electronic properties may further decrease the stability of the Pt(II)/Pt(IV) complexes and lower the activation energy required for the formation of Pt(II) σ-complexes and for the elimination of hydrocarbons from Pt(IV) alkyl hydrides.

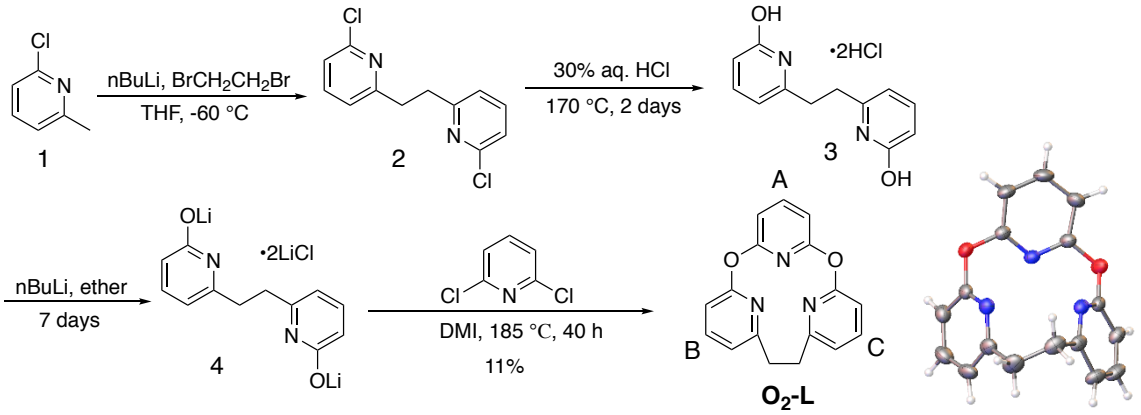

Scheme 5: The preparation of O_2-L. Each of the first 3 steps has near quantitative yield. The last step is an equilibrium reaction accompanied by polymerization.

The synthesis of O_2-L is shown in Scheme 5. The preparation of O_2-L is very different from that of L though the two ligands only differ at the bridging groups. 1,2-bis(6-chloropyridin-2-yl)ethane (**2**) was formed by reacting 6-chloro-2-picoline **1**, deprotonated

by *n*BuLi at -60 ℃, with 0.5 eq. bromination reagent 1,2-dibromoethane. The product **2** was dissolved in excess 30% HCl and heated at 170 ℃ in a sealed Schlenk tube to give bis-pyridone **3** in quantitative yield in 2 days. The lithium salt **4** derived from **3** was heated with 2,6-dicholropyridine in 1,3-dimethyl-2-imidazolidinone (DMI) at 185 ℃ over 40 h to afford the macrocycle O_2-L in 11% isolated yield.

Single crystal X-ray diffraction of O_2-L reveals that none of the pyridine rings are on the same plane with the three nitrogen atoms. Similar to L, the three nitrogen atoms are not able to bind to a metal simultaneously in square planar complexes. The pyridyl rings may reorient to accommodate facial coordination in octahedral complexes, however, the associated strain energy could result in considerable destabilization of the complexes.

2.2 Coordination of O_2-L with Transition Metals

Reaction of O_2-L with $PdCl_2(NCMe)_2$ at 50 °C in acetonitrile, followed by overnight cooling at room temperature, gives pure (O_2-L)$PdCl_2$ as reddish powder (Figure 3a). ^{1}H NMR of (O_2-L)$PdCl_2$ (Figure 3b) in CD_2Cl_2 at 22 °C shows a triplet for the para hydrogen of the central pyridine ring (A ring) and a doublet for the two meta hydrogens of the central ring. The hydrogens on ring B and C appear as a triplet (para H's, integral is 2) and two partially overlapping doublets (meta H's, overall integral is 4). Interestingly, the ethylene moiety appears as two broadened singlets (integral is 2 for each), suggesting of a fluxional behavior of the complex (O_2-L)$PdCl_2$ at 22 ^{o}C. It is proposed that the palladium atom migrates rapidly between nitrogens of the B and C rings of the ligand while maintaining bonding to the nitrogen of the ring A. At -40 °C, the broadened singlets become resolved as multiplets, including three triplets (para H's), six doublets (meta H's), and two sets of

complex multiplets (ethylene moiety). It is inferred from the VT NMR spectrum that the structure of the complex has C_1 symmetry.

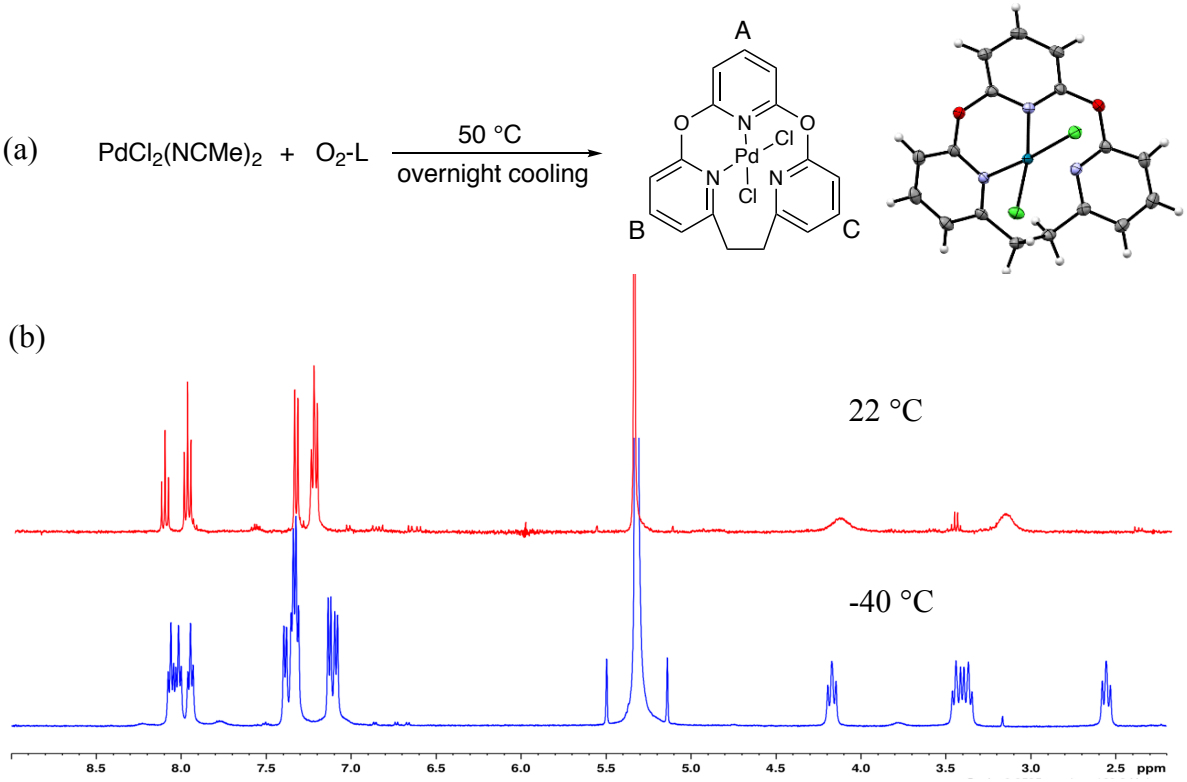

Figure 3: (a) The preparation of $(O_2\text{-L})PdCl_2$ and the X-ray diffraction structure of the product. Selected bond lengths and angles: Pd-N1, 2.0408 Å, Pd-N2, 2.0499 Å; Pd-N3, 2.8787 Å ; Pd-Cl1, 2.2786 Å; Pd-Cl2, 2.2925 Å; N1-Pd-N2, 83.88; N1-Pd-N3, 66.98; N2-Pd-N3, 80.19; N1-Pd-Cl1, 171.23; N1-Pd-Cl2, 92.25; N2-Pd-Cl1, 91.78; N2-Pd-Cl2, 175.32; Cl1-Pd-Cl2, 91.71. N1, N2, N3 are respectively the N atoms on the A, B, C pyridyl rings; Cl1 is the lower Cl atom on the graph, Cl2 is the higher one. (b) ^{1}H NMR spectra of $(O_2\text{-L})PdCl_2$ at 22 °C and -40 °C. The spectrum at 22 °C exhibits fewer peaks including two broad singlets for the ethylene moiety between 3.0 and 4.5 ppm; the spectrum at -40 °C exhibits resolved multiplets that correspond to the unsymmetric isomer of $(O_2\text{-L})PdCl_2$.

The inference was confirmed by the X-ray diffraction structure of $(O_2\text{-L})PdCl_2$, which shows that the complex coordination unit adopts a near-planar geometry, with the Pd atom bonding to N(A) and N(B) with roughly equal bond lengths (2.0408 Å and 2.0499 Å) and an angle of 83.88°. Nevertheless, the ring constraints of O_2-L leave the face of the C ring above the $PdCl_2$ plane. The distance from N(C) to Pd is 2.878 Å and the lone pair of N(C)

orients away from Pd.

With such a small distance between Pd and the C ring, it is believed that a repulsive interaction exists between the filled Pd d_{z^2} orbital and the C ring π-electrons (or electrons of the nitrogen lone pair). The d_{z^2}/π-cloud repulsion is not a newly discovered feature of the system -- it has been reported for the complex $LPdCl_2$ before[13]. This repulsion also helps in explaining the preference for *uns*-$(O_2\text{-L})PdCl_2$ over its C_s-symmetrical isomer. The distance between Pd and the out-of-plane N is expected to be smaller in the C_s-symmetrical isomer than in the C_1-symmetrical isomer because of the shorter tether (O vs. ethylene) to the pendant pyridyl group. The smaller distance will result in a significantly higher d_{z^2}/π-cloud repulsion and consequently a strong destabilization of the symmetric isomer. In agreement with the observed geometric preference, our DFT calculations show that the C_1-symmetric form of $LPdCl_2$ is favored over its symmetrical isomer by a $\Delta G°$ of 5.6 kcal/mol.

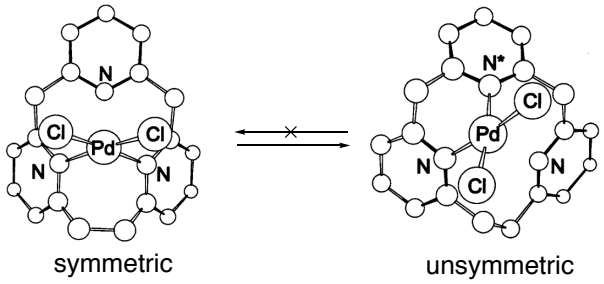

Figure 4: Symmetric and unsymmetric isomers of $(O_2\text{-L})PdCl_2$. The symmetric isomer is favored.

It's worth noting that $(O_2\text{-L})PdCl_2$ is of very low solubility in most solvents. Only 0.6 mg of the complex was dissolved in 1 mL DCM at 20 ℃ and the solubility is not better in other common solvents (ether, EtOAc or MeCN, etc.). A possible explanation for the low solubility is the strong intermolecular π-π stacking interactions between the pyridyl rings. The solubility issue is even worsened for $(O_2\text{-L})NiCl_2$ and $(O_2\text{-L})CuCl_2$, which were prepared using the same procedure as was $(O_2\text{-L})PdCl_2$. The formation of $(O_2\text{-L})NiCl_2$ and

(O_2-L)$CuCl_2$ was confirmed by the color change (blue to bright green for (O_2-L)$CuCl_2$ and light yellow to light blue for (O_2-L)$NiCl_2$) and the disappearance of the free ligand NMR signals in the reaction mixtures. However, due to the solubility issues, the characterization of the products has not been successful.

(O_2-L)CuCl was prepared by mixing CuCl and O_2-L in degassed DCM. Different from (O_2-L)$PdCl_2$, (O_2-L)CuCl dissolves well in organic solvents. ^{1}H NMR of (O_2-L)CuCl in d_2-DCM at room temperature displays broadened singlets for a majority of the ligand protons, with the exception that the para hydrogen of the central pyridine ring (A ring) appears as a sharp triplet (Figure 5). The spectrum is in agreement with a structure where the Cu atom migrates rapidly between nitrogens of the B and C rings of the ligand. We propose that at low temperature (O_2-L)CuCl will adopt a trigonal planar geometry, as has been found for many other Cu(I) complexes.

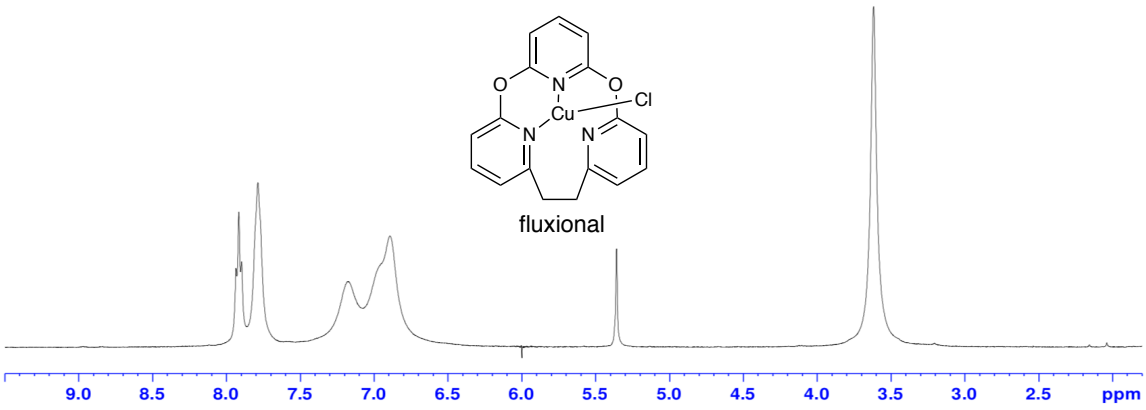

Figure 5: Broadened ^{1}H NMR signals indicate that the structure of (O_2-L)CuCl is fast-fluxioning.

Finally, our efforts towards the synthesis of (O_2-L)$PtCl_2$ were not successful. Acetonitrile coordinates very strongly with Pt in $PtCl_2(NCMe)_2$, and thus cannot be displaced by O_2-L at temperatures up to 80 °C. We also tried the reaction of $PtCl_2(NMe_3)_2$ with O_2-L, but only the starting materials were recovered.

2.3 Direct Olefin Aziridination Catalyzed by $(O_2\text{-L})Cu^+$

The catalytic activity of LCu^+ in the reaction between substituted aliphatic olefins and PhINTs to afford aziridines, reported by Vedernikov in 2003[28], was quite impressive. The catalyst LCu^+ was prepared from the precursor LCuCl by chloride abstraction with $NaBArF_4$ in anhydrous DCM. Luckily, the same procedure can be applied to obtain $(O_2\text{-L})Cu^+$ (eq. 3), which is also fluxional and only two-coordinate according to its ^1H NMR sepectrum. $(O_2\text{-L})Cu^+$ is stable for up to a month at -20 ℃ in DCM in the absence of a substrate.

$$(O_2\text{-L})CuCl + NaBArF_4 \xrightarrow{DCM} (O_2\text{-L})Cu^+\ BArF_4^- + NaCl \qquad (3)$$

In analogy to the previous work using LCu^+, our initial effort to make an aziridine with $(O_2\text{-L})Cu^+$ involved 5 mol% catalyst loading (vs PhINTs) and excess of cis-cyclooctene (3 eq.). The reaction was carried out at room temperature in a glovebox and the yield was excellent (>98%). When the catalyst loading was decreased to 2.5 mol% and cis-cyclooctene decreased to 1.2 eq, the product was still furnished in 90% yield. It's observed that once the olefin is added to the mixture of PhINTs and $(O_2\text{-L})Cu^+$, the color of the solution quickly changes from light yellow (the color of $(O_2\text{-L})Cu^+$) to deep green, indicating an oxidation of Cu(I) to Cu(II). The same observation was reported and discussed in the previous work for LCu^+. The discussion concluded that the color change is due to the quantitative stoichiometric oxidation of LCu^+ by PhINTs to the dinuclear copper(II) complex $[(LCu^{II})_2NTs]^{2+}$, which was successfully characterized by ^1H and ^{13}C NMR spectroscopy[28]. However, it's unclear whether this dinuclear copper(II) complex or the unoxidized Cu(I) complex is the active catalyst in the aziridination reaction.

Having achieved a satisfactory initial result, we next evaluated the scope of the aziridination protocol (Scheme 6). Cycloheptene delivered the corresponding aziridine in 90% NMR yield at 0 °C in the presence of 2.5 mol% catalyst. Cyclohexene and cyclopentene afforded slightly lower yields, 80% and 78% respectively, even though the catalyst loading was doubled. The lower yields were possibly resulted from significant amount of α-amination at the secondary allylic CH bonds, a side reaction that has been observed before. This method is not limited to 1,2-disubstituted substrates; mono-, tri- and tetra- substituted olefins were also viable aziridination partners, as evidenced by the (near)

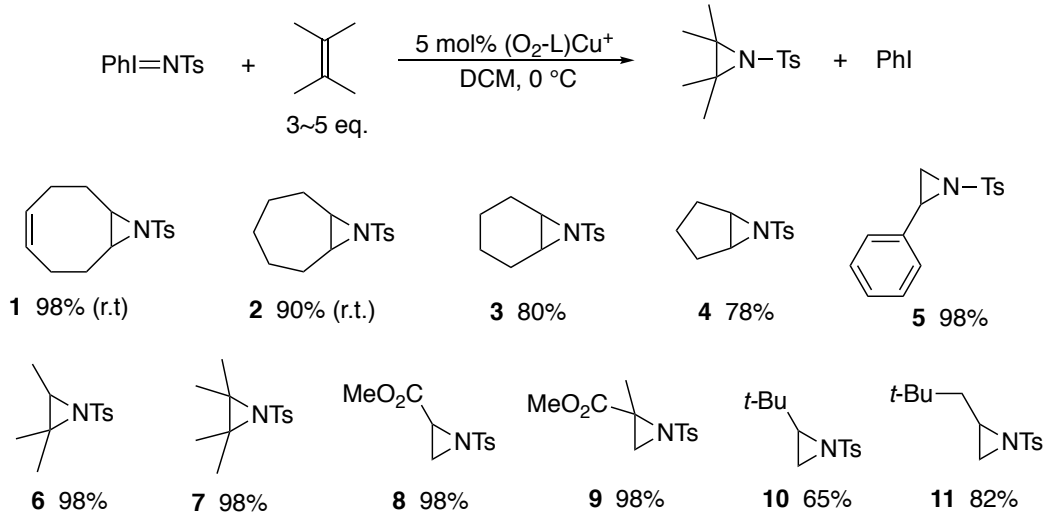

Scheme 6: Substrate scope for the direct aziridination reaction catalyzed by 5 mol% $(O_2\text{-L})Cu^+$. All yields are NMR yields w.r.t. liberated PhI.

quantitative formation of **5**-**7**. In addition, the protocol was successful for olefins bearing electron-withdrawing groups on the C=C bond, furnishing **8** and **9** in excellent yields. The formation of **9** also demonstrated the suitability of this method for 1,1-disubstituted olefins. It was found that steric bulk adjacent to C=C bond significantly inhibits the reaction, as indicated by the significantly lower yield of **10**. The t-butyl group on H_2C=CH-*t*Bu could orient toward the pendent pyridyl ring of ligand O_2-L and consequently prevent the

coordination of the catalyst with the olefin. Adding a CH_2 between the double bond and the t-butyl group led to a considerable increase in yield (**11**), probably because the CH_2 allows more flexibility for the substituent's orientation and thus reduces the van der Waals repulsion.

Due to the limited number of results achieved so far, it is premature to compare the catalytic performance of $(O_2\text{-L})Cu^+$ with LCu^+, however, it is safe to say that both of them are among the most efficient direct aziridination catalysts[22,26-27]. Summarized in table 1 are the performances of 10 other transition metal complexes in direct olefin aziridination, using styrene as the olefin substrate and PhINTs as the nitrene source.

Table 1. Transition-metal-catalyzed intermolecular aziridination of styrene with PhINTs.

Entry	Catalyst[a]	Yield[b](%)	Ref.
1	[Tp′Cu(C_2H_4)] (**12**), 5 mol%	90	29
2	CuHY (Y= zeolite), 25 mol%	90	30
3	copper(I) β-diketiminate (**13**), 5 mol%	85[c]	31
4	[(i-Pr_3TACN)Cu(O_2CCF_3)$_2$] (**14**), 5 mol%	95	32
5	Fe(OTf)$_2$, 5 mol%	82	33
6	[Fe(terpy)$_2$][ClO_4]$_2$ (**15**), 5 mol%	96[c,d]	34
7	[(η5-C_5H_5)Fe(CO)$_2$(THF)][BF_4] (**16**), 10 mol%	85	35
8	[{(3,5-$(CF_3)_2$Pz)ZnEt}$_2$(μ-THF)] (**17**), 5 mol%	68	36
9	[Ag_2(tBu_3tpy)$_2$(NO_3)](NO_3) (**18**), 2 mol%	91	37
10	[Ru(F_{20}-TPP)(CO)] (**19**), 1.5 mol%	86[c,e]	38

[a] see Figure 6 for the structures of the catalysts [b] the product is **5** and yields are isolated unless otherwise specified; [c] GC or NMR yield; [d] based on 86% conversion; [e] based on 82% conversion.

$(O_2\text{-L})Cu^+$ and LCu^+, furnishing the product **5** in near quantitative yields, show catalytic activities that compete with the best of the above-listed complexes. In addition, reactions

catalyzed by $(O_2\text{-L})Cu^+$ and LCu^+ are complete in only minutes at 0 °C. Though 5 mol% catalyst was used in most of the examples, evidence has shown that the catalyst loading may be reduced significantly while the yield stays the same (1 mol% LCu^+ furnished 98% of the aziridination product from cyclooctene).

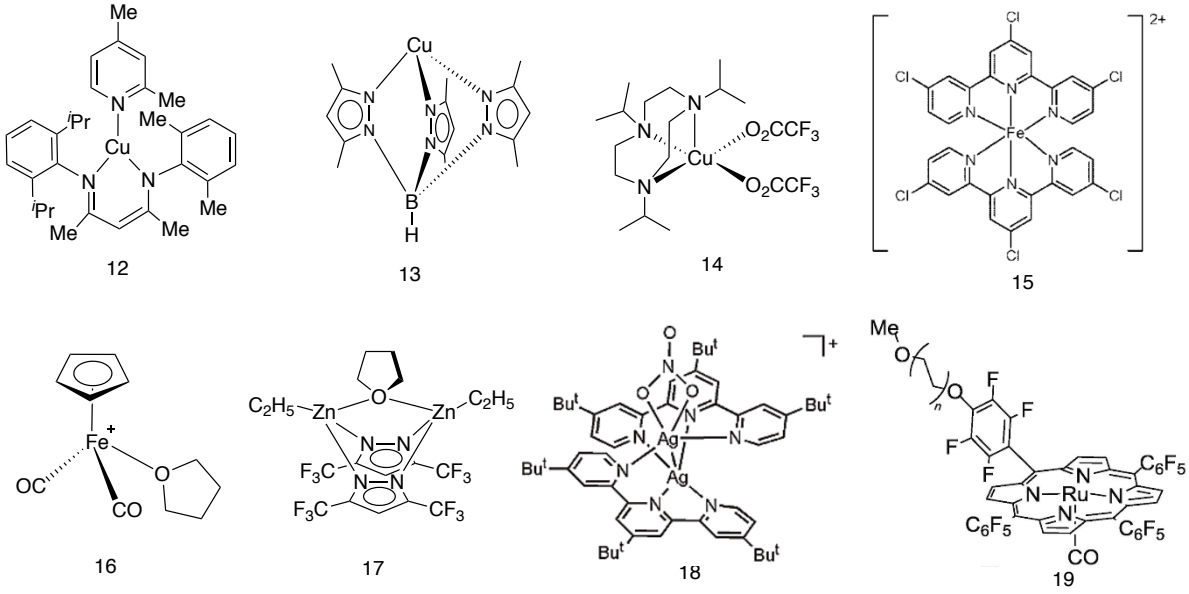

Figure 6: Selected other transition metal catalysts for direct olefin aziridination.

2.4 C-H Activation with $[LPtH_2Me]^+$

$[LPtH_2Me]^+$ (see Figure 2a for **L**; counterion $BArF_4^-$) was prepared following the published procedures (Scheme 7)[10].

Single crystal X-ray diffraction of $[LPtH_2Me]^+$ shows that the ligand L binds facially with Pt, and one of the two hydrides coordinates trans to the A ring of L while the other coordinates trans to the B/C ring. In agreement with the solid state structure, ^1H NMR of $[LPtH_2Me]^+$ shows two separate resonance signals for nonequivalent hydrido ligands at d = 20.37 (s, $^1J_{Pt\text{-}H}$ = 1318 Hz) and 19.32 ppm (s, $^1J_{Pt\text{-}H}$ = 1276 Hz) (CD_2Cl_2, 21°C), two sets of signals with an AX pattern for the ligand methylene bridges, three triplets for para

protons of pyridine residues in a 1:1:1 ratio, and six doublets for the corresponding meta protons of equal intensity.

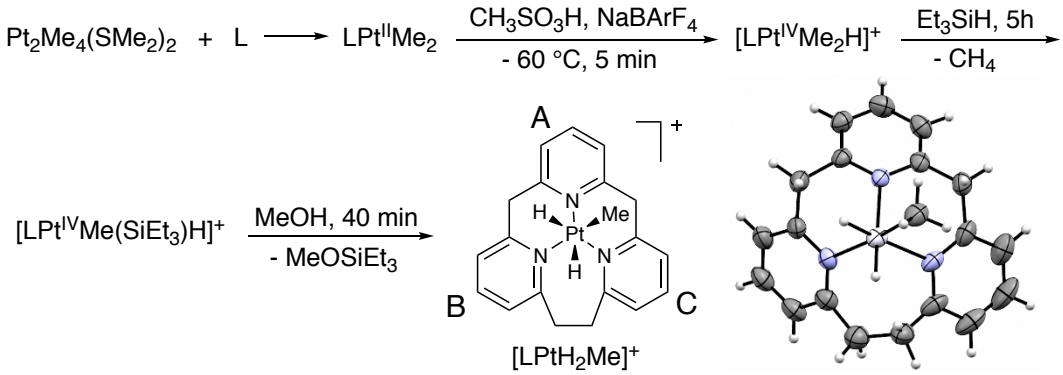

Scheme 7: The preparation of $[LPtH_2Me]^+$ and the X-ray diffraction structure of the product.

Calculated free energies for methane and for H_2 elimination from $[LPtH_2Me]^+$ have been reported before (DFT, PBE functional, SBK basis set, and program package Priroda; Figure 7). The calculation reveals that methane elimination is easier to achieve than elimination of H_2, both thermodynamically and kinetically, by more than 13 kcal/mol. The calculation also demonstrates that the transient $[LPtH]^+$ does not adopt the planar four-coordinate configuration preferred by Pt^{II} due to the structural constraints of ligand L; instead, the Pt(II) complex acquires a three-coordinate T-shaped geometry, with only 14 valence electrons. The out-of-plane pendant N atom interacts negligibly with the Pt^{II} center.

When $[LPtH_2Me]^+$ was heated in a solution of DCM containing benzene (50 vol%) in a sealed NMR tube at 86 °C, the NMR signals of the methyl ligand and both hydride ligands of the starting complex gradually diminished while two new hydride signals appeared at d = 19.51 (s, $^1J_{Pt\text{-}H}$ = 1349 Hz) and 18.38 ppm (s, $^1J_{Pt\text{-}H}$ = 1307 Hz) (CD_2Cl_2, 21 °C. Figure 8). In 8 hours, the starting complex transformed almost quantitatively into $[LPtH_2Ph]^+$, which possesses the same low symmetry as its methyl predecessor.

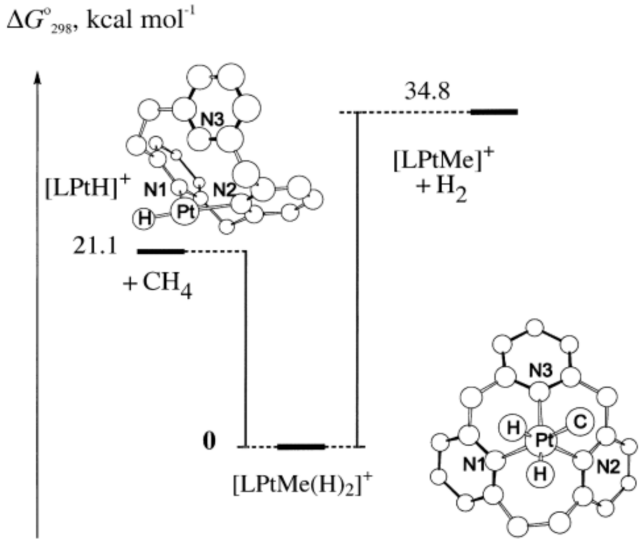

Figure 7: DFT-calculated Gibbs free energy [kcalmol^{-1}] of methane versus dihydrogen elimination from $[LPtMeH_2]^+$. Selected bond lengths [Å]: $[LPtH]^+$: Pt-N1 1.991, Pt-N2 2.173, Pt-N3 2.985; $[LPtMe(H)_2]^+$: Pt-N1 2.243, Pt-N2 2.243, Pt-N3 2.222.

When the same protocol was applied to para-xylene, decomposition of $[LPtMeH_2]^+$ was observed without concomitant formation of new Pt(IV) hydrides. The degradation was presumably caused by side reactions with DCM or undesired CH activations at the bridging methylene groups of the ligand L. We next examined the reactions between $[LPtMeH_2]^+$ and meta-xylene/ortho-xylene. Luckily in both cases we observed the appearance of new hydride signals, together with the gradual diminution of the methyl ligand peaks, which suggests that the desired dihydrido aryl complexes were formed (72% NMR yield for meta-xylene, 75% for ortho-xylene). The appearance of only two new hydride signals for each reaction demonstrates that CH activation at meta-xylene and ortho-xylene occurred regio-selectively. This inference is further supported by the observation that, in the reaction with meta-xylene, the two xylene methyl groups appear as only one singlet on the ^{1}H NMR spectrum.

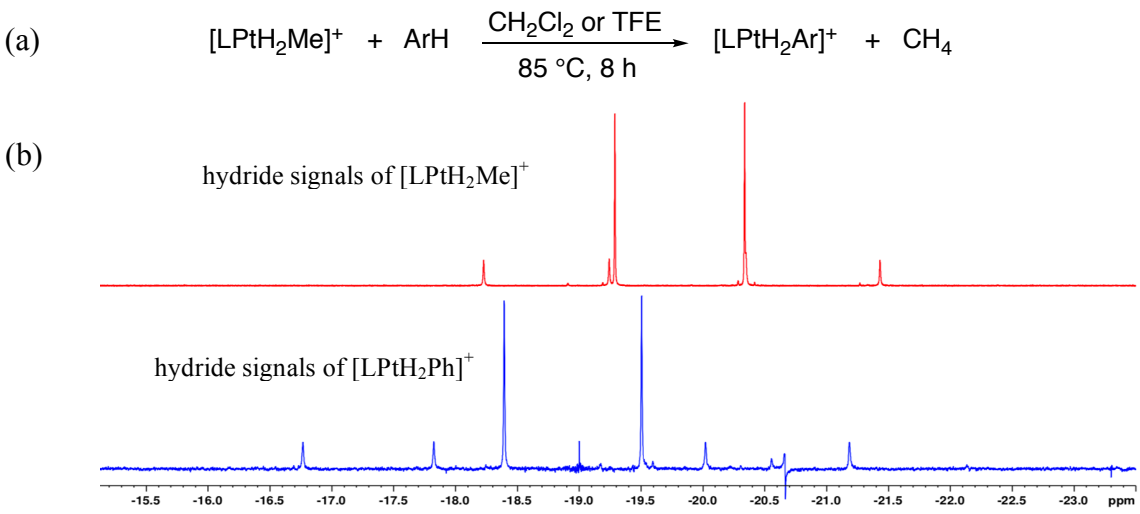

Figure 8: (a) $[LPtH_2Me]^+$ when heated in arenes cleaves the aryl CH bonds and produces $[LPtH_2Ar]^+$; (b) $[LPtH_2Ph]^+$ and $[LPtH_2Me]^+$ share the same pattern of hydride signals, indicating that they possess the same molecular symmetry.

It is therefore concluded that sterics play an essential role in the CH activation reactions using $[LPtMeH_2]^+$. The CH bonds that are furthest from the substituents on the arenes get cleaved preferentially. If no meta- or para- (relative to the substituents) CH bonds are available, only decomposition of the Pt complex will occur.

Given the above conclusion, it is within expectation that the reaction of $[LPtMeH_2]^+$ with para-difluorobenzene did not go well. Meta-difluorobenezene, in contrast, gives a single CH activation product at 70% yield after 8 hours. This result is interesting because it is one of the rare examples where electron-poor CH bonds get cleaved efficiently. The reaction of ortho-difluorobenzene with $[LPtMeH_2]^+$ afforded fluxional products, which was evidenced by the appearance of broadened signals in the ^1H NMR spectrum of the crude product; at low temperature the spectrum resolved to 3 sets of peaks, indicating the formation of unidentified side products.

To learn more about the above reactions, we heated $[LPtMeH_2]^+$ with benzene in TFE-d_1

at 85 °C. Same as the reaction in DCM, the Pt(IV)-phenyl complex was formed almost quantitatively in 8 hours. However, the product produced in d1-TFE gave neither hydride signals nor phenyl proton signals, revealing the occurrence of a complete and fast H/D exchange (eq. 4). This observation tells us that, at the most conservative analysis, CH bond cleavage at the Pt-PhH σ-complex and reformation of the σ-complex from the CH cleavage product are facile processes at the protocol condition.

$$[LPtH_2Me]^+ + PhH \xrightarrow[85\ °C,\ 8\ h]{CF_3CH_2OD} [LPt(C_6D_5)D_2]^+ + CH_4 \quad (4)$$

$$[LPtH_2Ph]^+ + m\text{-}C_6H_4F_2 \xrightarrow[85\ °C,\ 8\ h]{CF_3CH_2OH} [LPt(m\text{-}C_6H_3F_2)H_2]^+ + PhH \quad (5)$$

$[LPtH_2Ph]^+$ was recovered after heating

We then attempted the reaction of $[LPtPhH_2]^+$ with pure meta-difluorobenzene at the same temperature (eq. 5). ^1H NMR demonstrated only little change (which is likely due to decomposition) of the staring complex over the 8-hour heating, suggesting that the displacement of benzene from the Pt-PhH σ-complex by m-$C_6H_4F_2$ is associated with high energy barrier. Assuming that formation of the 3-coordinate transient species $[LPtH]^+$ is required to easily coordinate with the surrounding m-$C_6H_4F_2$ molecules and subsequently afford the CH activation product $[LPt(C_6H_3F_2)H_2]^+$, we conclude that the dissociation of benzene from the Pt-PhH σ-complex is rate limiting step.

The above conclusion is consistent with results of concurrent CH activation experiments where $[LPtMeH_2]^+$ was reacted with a benzene/m-$C_6H_4F_2$ mixture(1:6.6 in volume, 1:1 with respect to reactive CH bonds). At 85 °C, the two expected $[LPtAr(H)_2]^+$ products were formed concurrently with a constant products ratio (Pt-Ph: Pt-$C_6H_3F_2$ = 1:2.48), regardless

of the reaction time (Figure 9). The constant product ratio revealed that the activation energy required for the dissociation of m-$C_6H_4F_2$ from the Pt-(m-$C_6H_4F_2$) σ-complex is also quite high, since otherwise the complex $[LPt(C_6H_3F_2)H_2]^+$ can be gradually turned into $[LPtPhH_2]^+$ (or vice versa) and the ratio would change over time.

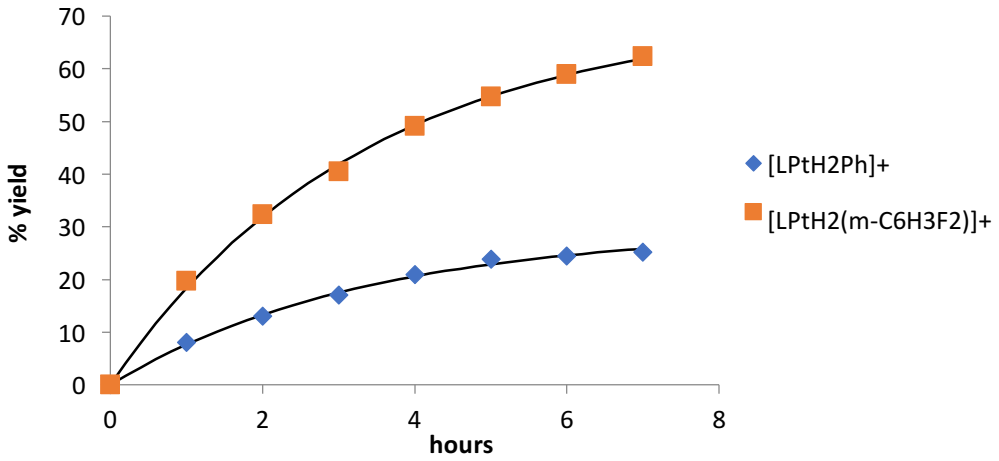

Figure 9: The reaction of $[LPtMeH_2]^+$ with a benzene/m-$C_6H_4F_2$ mixture gives the two products in a constant ratio of 1:2.48. The ratio is pure kinetic because the high activation energy required for the dissociation of arenes from σ-arene complexes prevents the reverse reactions.

Though we used benzene and m-$C_6H_4F_2$ for the demonstration, it is reasonable to propose that the dissociation of methane from the σ-complex $[LHPt\text{-}CH_4]^+$ is also associated with high energy barrier and is rate-limiting in the conversion of $[LPtMeH_2]^+$ to $[LPtH]^+$ plus free CH_4. DFT calculations were carried out to support the hypothesis (Figure 10). The computation shows that the formation of $[LHPt\text{-}CH_4]^+$ (**T1**) from $[LPtMeH_2]^+$ overcomes a barrier of 17.4 kcal/mol; the afforded σ-complex **I1** has an energy of 14.7 kcal/mol. To produce the transient intermediate $[LPtH]^+$ (**I2**), an overall enthalpy change of +33.9 kcal/mol is required, which is, numerically, the upper limit for the $\Delta G^{\ddagger}$ of its production in the ultimate case of $T\Delta S^{\ddagger} = 0$ (purely dissociative loss of CH_4). $[LPtH]^+$, at $\Delta G = 19.2$ kcal/mol, stands as the most high-energy intermediate in the reaction. $[LPtH]^+$ then easily

coordinates with the arenes and cleaves their CH bonds. The final products are more stable than the starting material by large energy differences (-11.1 kcal/mol for $[LPtPhH_2]^+$ and -8.6 kcal/mol for $[LPt(m\text{-}C_6H_3F_2)H_2]^+$), compared to ArH + $[LPtMeH_2]^+$, agreeing with the experimental observations that higher activation energy is required for arene eliminations than for methane elimination.

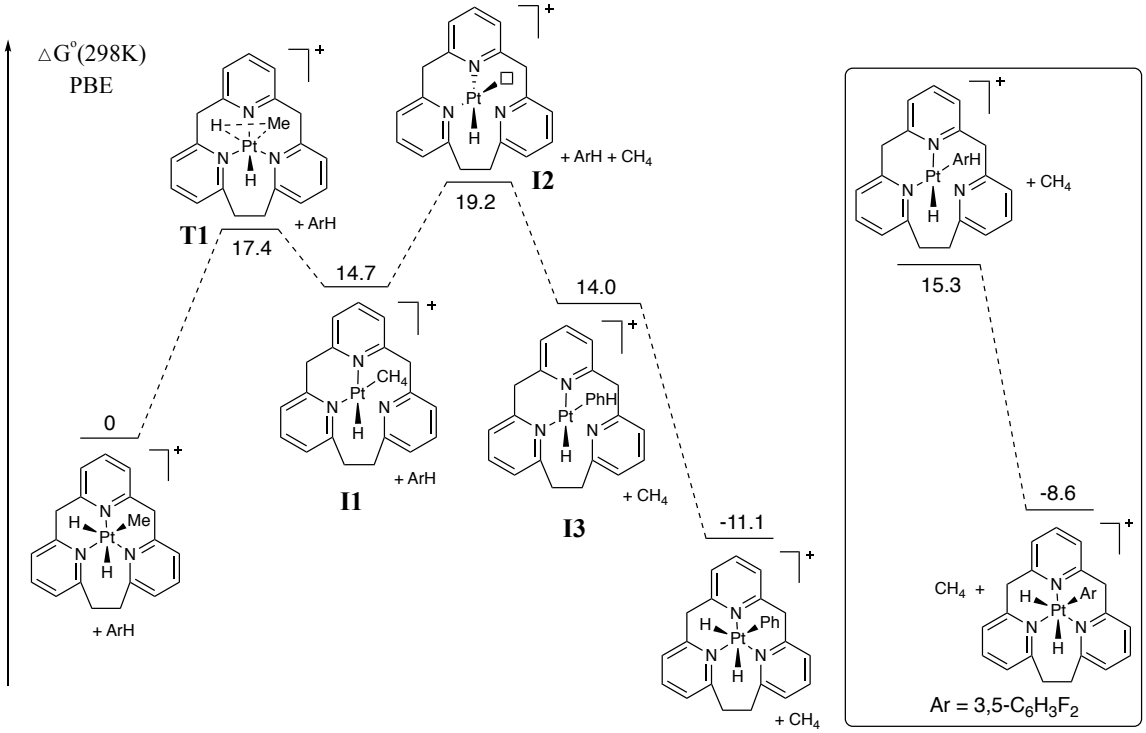

Figure 10: Calculated Gibbs free energies for the conversion of $[LPtMeH_2]^+$ to $[LPtArH_2]^+$.

2.5 Conclusions and Future Work

As part of our lab's efforts to discover efficient catalysts that promote C-H bond activation/ oxidative functionalization of un-activated hydrocarbons, we prepared the constrained macrocycle O_2-L, an analogue of the previously reported ligand L. The three nitrogen atom donors on O_2-L can (poorly) adapt to the octahedral geometry prefer by d^6 transition metals but cannot arrange a coplanar coordination to accommodate the square-planar geometry

preferred by d^8 metals. Studies of the d^8 complex $(O_2\text{-L})PdCl_2$ reveals that only two of the three nitrogen atoms in O_2-L bind to the metal; the Pd atom migrates quickly between the two nitrogen atoms tethered by the ethylene linkage at room temperature. The complex $(O_2\text{-L})Cu^+$ exhibited outstanding performance in promoting direct aziridination reactions; the aziridine products were yielded near quantitatively in the absence of bulky substituents next to the C=C bonds.

Mechanism and substrate scope of the previously reported C-H activation protocol using $[LPtH_2Me]^+$ have been briefly explored. The method was found very sensitive to the steric hindrance caused by substituents on the hydrocarbon substrates. No cleavage of C-H bonds next to the substituents on arenes has been observed in the reaction. On the other hand, this sensitivity to sterics resulted in exceptional regioselectivity: only one product was formed in the reaction of $[LPtH_2Me]^+$ with meta- or ortho- disubstituted benzenes. Mechanistic studies suggest that C-H bond cleavage in the Pt^{II}-alkane/arene σ-complex is facile and reversible at 85 ℃. However, the dissociation of an alkane or arene molecule from the Pt^{II}-alkane/arene σ-complex generally requires high activation energy and is rate-limiting.

A future direction of this work is to fine-tune the steric and the electronic properties of the ligand to improve the efficiency of the C-H activation protocol. The near goal is to lower the reaction temperature and to slow down (or prevent) the decomposition of the products. The ligand O_2-L is potentially an improvement over ligand L for this purpose. Regrettably, efforts toward the preparation of $[(O_2\text{-L})PtH_2Me]^+$ has not achieved a success so far. The development of a working synthetic route to $[(O_2\text{-L})PtH_2Me]^+$ will be continued in our lab in the future.

Supplemental Materials

General Information

All manipulations with air and moisture sensitive compounds were carried out under purified Ar atmosphere using standard Schlenk or glovebox techniques. All solvents and liquid reagents were dried (activated 3Å or 4Å molecular sieves for hydrocarbons and trifluoroethanol, Na/benzophenone for ether and THF, CaH_2 for dichoromethane and acetonitrile) and vacuum-transferred or distilled under Ar prior to use. $[LPtH_2Me][BArF_4]$ and PhINTs was prepared according to the previously reported literature procedures in similar yields and purity. All reagents that are not synthesized in our lab were purchased from Sigma-Aldrich, Alfa Aesar, Ark Pham, Oakwood Chemical, and used as received unless otherwise stated. All ^{1}H NMR and ^{13}C NMR spectra were recorded at Bruker AV-400, Bruker DRX-500 and Bruker AVIII-600 spectrometers. Chemical shifts are reported in ppm and referenced to residual solvent peaks. Coupling constants are reported in Hz and indicate ^{1}H-^{1}H coupling unless otherwise noted. Low temperature NMR data involved calibration with methanol standards. All mass spectra were analyzed on a JEOL AccuTOF-CS mass spectrometer using electron spray ionization in the positive mode for the detection of ions. ESI-MS were compared with mass calibration standards and most intense peaks were reported. X-ray structures were solved by Dr. Peter Zavalij and are displayed as ORTEP drawings with 50% probability ellipsoids. DFT calculations were performed by Dr. Andrei Vedernikov using Priroda/Jaguar program and PBE/PBE-D3 models.

Synthesis

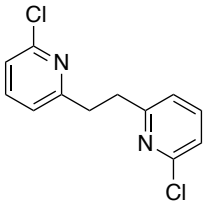

1,2-bis(6-chloropyridin-2-yl)ethane (2)

An oven-dried 250 mL round bottom flask was charged with a magnetic stir bar and Ar. To the capped flask was injected 150 mL anhydrous THF and 15 mL (0.15 mol) anhydrous 6-chloro-2-picoline. The stirred solution was cooled at -60 ℃, and then 13.7 mL of a 11.0 M n-butyllithium solution in hexanes (0.15 mol) was added with a syringe over 20 minutes. The resulting dark red solution was stirred at -60 ℃ for 1 additional hour before being further cooled to -78 ℃. A solution of 6.5 mL (0.075 mol) of 1,2-dibromoethane in 10 mL THF was then injected with a syringe over 10~20 minutes. When the addition was complete, the mixture turned light red and was then allowed to naturally warm up to room temperature (overnight). The solution became colorless. A saturated aqueous solution of potassium hydroxide (20 g) was added to the reaction and the mixture was swirled thoroughly. The resulting almost colorless liquid was decanted from a precipitate of lithium hydroxide and potassium bromide and dried overnight over solid potassium hydroxide. After removal of the solvent and distillation under vacuum, pure 1,2-bis(6-chloropyridin-2-yl)ethane was obtained (13.7 g, 93%) as a colorless crystalline solid.

^{1}H NMR (400 MHz, $CDCl_3$, 22 ℃) δ 7.52 (t, J = 7.7 Hz, 2H), 7.15 (dd, J = 7.9, 0.9 Hz, 2H), 7.05 (dd, J = 7.6, 0.9 Hz, 2H), 3.20 (s, 4H).

ESI-MS calcd. for $C_{12}H_{11}Cl_2N_2^+$ $[M+H]^+$ 252.02, found 252.04.

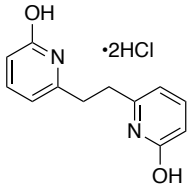

1,2-bis(6-hydroxypyridin-2-yl)ethane bis(hydrogen chloride) (3)

6.6g 1,2-bis(6-chloropyridin-2-yl)ethane (2) was dissolved in 25 mL 30% aqueous HCl

solution, then the solution was transferred to a 50 mL Schlenk tube and sealed. The reaction was then heated in silicon oil bath at 170 ℃ over 40 hours. In the first 10 hours the Schlenk tube was removed from oil bath and cooled to room temperature then uncapped to release the pressure (the reaction consumes H_2O and produces HCl, so the pressure builds up inside) every 2 hours. After the first 10 hours the pressure was released every 5 hours. After 40 hours of heating the reaction was cooled to room temperature and the solution was transferred to a round bottom flask. The excess HCl solution was then removed on a rotavapor and on high vacuum to give compound 3 quantitatively as an off-white crystalline solid, which was used in next step without further purification.

^{1}H NMR (400 MHz, CD_3OD, 22 ℃) δ 8.16 (dd, J = 8.8, 7.4 Hz, 2H), 7.10 (d, J = 7.4 Hz, 2H), 7.06 (d, J = 8.8 Hz, 2H), 3.28 (s, 4H).

^{13}C NMR (151 MHz, CD_3OD, 22 ℃) δ 163.12, 151.26, 116.20, 113.51, 32.48.

ESI-MS calcd. for $C_{12}H_{13}N_2O_2^+$ $[M+H]^+$ 217.10, found 217.14.

Lithium 6,6'-(ethane-1,2-diyl)bis(pyridin-2-olate) (4)

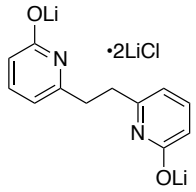

To an oven-dried 500 mL round bottom flask was charged a stir bar, 7.18g (33 mmol) compound 3 and 200 mL anhydrous diethyl ether. The flask was sealed under argon. Then 3.0 mL of a 11.0 M n-butyllithium solution in hexanes was injected to the suspended solution via syringe. The reaction was stirred under Ar for a week. The solvent was then carefully removed on a rotavapor and the residual was dried on high vacuum to afford the product 4 in quantitative yield as fine white powder.

^{1}H NMR (400 MHz, CD_3OD, 22 ℃) δ 7.26 (dd, J = 8.5, 7.0 Hz, 2H), 6.23 (td, J = 8.2, 0.9 Hz, 4H), 2.82 (s, 4H).

[2.1.1]-(2,6)-9,16-dioxapyridinophane (O_2-L)

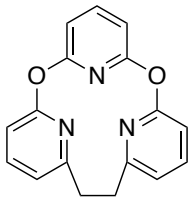

11.56 g (37 mmol) of the lithium salt 4 was dissolved in 120 mL pre-dried 1,3-Dimethyl-2-imidazolidinone (DMI) in a 250 mL round bottom flask followed by the addition of 5.93g (40 mmol) 2,6-dichlorobenzene. The mixture was sealed under argon and heated at 185 ℃ over 3 days before cooled to room temperature and quenched by excess aqueous KOH solution. The quench reaction was diluted with 500 mL water and extracted with dichloromethane three times. After dichloromethane was evaporated on a rotavapor, the residual was distilled at 110 ℃ on high vacuum to remove DMI and then at 230 ℃ to collect the crude product, which was further purified by recrystallization in EtOAc and hexanes. The pure O_2-L was a white crystalline solid (1.31g, 12%) and was easily re-crystallized to give crystals suitable for single crystal X-ray characterization.

^{1}H NMR (600 MHz, $CDCl_3$, 22 ℃) δ 7.76 (t, J = 7.9 Hz, 1H), 7.46 (t, J = 7.7 Hz, 2H), 6.81 (dd, J = 7.5, 0.8 Hz, 2H), 6.76 (d, J = 7.9 Hz, 2H), 6.68 (dd, J = 7.9, 0.8 Hz, 2H), 3.24 (s, 4H).

^{13}C NMR (126 MHz, $CDCl_3$, 22 ℃) δ 161.72, 161.20, 158.63, 142.29, 139.21, 119.44, 111.06, 106.63, 35.82.

ESI-MS calcd. for $C_{12}H_{11}Cl_2N_2^+$ $[M+H]^+$ 292.11, found 292.20.

(O_2-L)$PdCl_2$

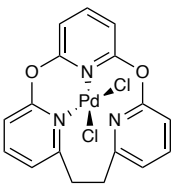

30.0 mg $PdCl_2$ was suspended in 3 mL pre-dried acetonitrile in a 10 mL Schlenk tube. The mixture was sealed and heated at 85 ℃ for 1 hour until all PdCl2 powder disappeared. The solution was then cooled to room temperature and 55.0 mg O2-L was added. The reaction was re-heated at 50 ℃ for 2 additional hours followed by being cooled to 0 ℃. The product crashed out of the solution as reddish powder and was collected by filtration. The wet powder was dried on high vacuum to give 80 mg (94%) of pure (O_2-L)$PdCl_2$. 9 mg of the product was dissolved in 15 mL DCM in an Erlenmeyer flask and sealed in a bottle that contained 30 mL pentanes. In a week crystals appeared on the wall of the Erlenmeyer flask. The crystals were handed to Dr. Peter Zavalij for single-crystal X-ray characterization.

^{1}H NMR (500 MHz, Methylene Chloride-d_2, -40 ℃) δ 8.06 (t, J = 8.1 Hz, 1H), 8.02 (t, J = 7.8 Hz, 1H), 7.95 (t, J = 7.9 Hz, 1H), 7.39 (d, J = 8.0 Hz, 1H), 7.33 (q, J = 7.8, 7.3 Hz, 3H), 7.13 (d, J = 8.2 Hz, 1H), 7.09 (d, J = 8.2 Hz, 1H), 4.17 (t, J = 12.1 Hz, 1H), 3.50 – 3.40 (m, 1H), 3.37 (t, J = 11.8 Hz, 1H), 2.55 (t, J = 12.0 Hz, 1H).

^{1}H NMR (400 MHz, CD_2Cl_2, 22 ℃) δ 8.12 (t, J = 8.0 Hz, 1H), 7.98 (t, J = 7.8 Hz, 2H), 7.35 (dd, J = 7.6, 1.1 Hz, 2H), 7.24 (t, J = 7.1 Hz, 3H), 4.15 (s, 2H), 3.17 (s, 2H).

ESI-MS calcd. for $C_{17}H_{14}Cl_2N_3O_2Pd^+$ $[M+H]^+$ 467.95, found 467.97.

See the “Crystal Data” section for the X-ray structure.

(O_2-L)CuCl

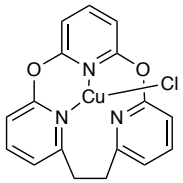

To an oven-dried 5 mL round bottom flask was charged 10.0 mg CuCl, 29.6 mg O2-L and 1 mL anhydrous & degassed dichloromethane in a glovebox. The mixture was stirred at

room temperature for 10 min and the product was formed quantitatively to give a yellowish DCM solution.

^{1}H NMR (400 MHz, CD_2Cl_2, 22 ℃) δ 7.92 (t, J = 7.9 Hz, 1H), 7.79 (t, J = 8.1 Hz, 2H), 7.52 – 6.18 (m, 6H), 3.62 (s, 4H).

General method for C-H activation with $[LPtH_2Me]^+$ $BArF_4^-$

$$[LPtH_2Me]^+ + ArH \xrightarrow[85\ °C,\ 8\ h]{CH_2Cl_2\ or\ TFE} [LPtH_2Ar]^+ + CH_4$$

13.6 mg $[LPtH_2Me]^+$ $BArF_4^-$ was charged to a Young's tube in a glovebox followed by the addition of 0.8 mL of the pre-dried and degassed hydrocarbon substrate (in DCM or TFE solution if the substrate is non-polar and does not dissolve the Pt complex well, in pure form if the substrate is polar). The mixture was sealed and heated at 85 ℃for 6~8 hours. ^{1}H NMR of the reaction mixture was taken after a sealed D_2O capillary tube was put into the Young's tube.

ArH = m-$C_6H_4F_2$

The reaction was carried out in pure m-$C_6H_4F_2$. After 7h the product $[LPtH_2(m\text{-}C_6H_3F_2)]^+$ $BArF_4^-$ was formed in 70% yield. 12% of the starting material $[LPtH_2Me]^+$ $BArF_4^-$ remained, according to the integral of the remaining Pt-Me ^{1}H NMR signals.

Hydride signals on the ^{1}H NMR spectrum (400 MHz, CD_2Cl_2, 22 ℃): -18.38 (d, $^1J_{Pt\text{-}H}$ = 1184, $^3J_{H\text{-}H}$ = 6.9), -19.45 (d, $^1J_{Pt\text{-}H}$ = 1218, $^3J_{H\text{-}H}$ = 7.6 Hz)

ArH = m-xylene

The reaction was carried out in 50% TFE solution. After 8h the product $[LPtH_2(m\text{-}C_6H_3(CH_3)_2)]^+$ $BArF_4^-$ was formed in 72% yield.

Hydride signals on the 1H NMR spectrum (400 MHz, CD_2Cl_2, 22 ℃): -18.17 (d, $^1J_{Pt\text{-}H}$ = 1308), -19.27 (d, $^1J_{Pt\text{-}H}$ = 1349)

ArH = o-xylene

The reaction was carried out in 50% TFE solution. After 8h the product $[LPtH_2(o\text{-}C_6H_3(CH_3)_2)]^+$ $BArF_4^-$ was formed in 75% yield.

Hydride signals on the 1H NMR spectrum (400 MHz, CD_2Cl_2, 22 ℃): -18.18 (d, $^1J_{Pt\text{-}H}$ = 1307), -19.28 (d, $^1J_{Pt\text{-}H}$ = 1349)

General method for olefin aziridination with $(O_2\text{-}L)Cu^+$ $BArF_4^-$

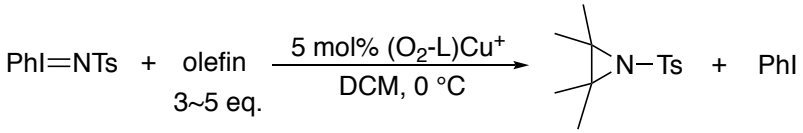

37.3 mg PhINTs, 3~5 equivalent of the olefin substrate and 0.6 mL degassed & anhydrous dichloromethane was charged to an oven-dried Young's tube under the protection of Ar. The Young's tube was gently shaken to make a suspension solution before being cooled to 0 ℃ in ice/water bath. Then 0.2 mL of a 25 mM $(O_2\text{-}L)Cu^+$ in dichloromethane solution was injected to the reaction. The color of the suspension solution changed to deep blue immediately as $(O_2\text{-}L)Cu^+$ was added, then after 1 to 5 minutes the color changed to green or deep green.

^{1}H NMR spectra data of the products **1-11** (see scheme 6) match well with those published in ref. 28&29. Yields were determined by comparing the integrals of the product signals to the integrals of liberated PhI.

Spectra

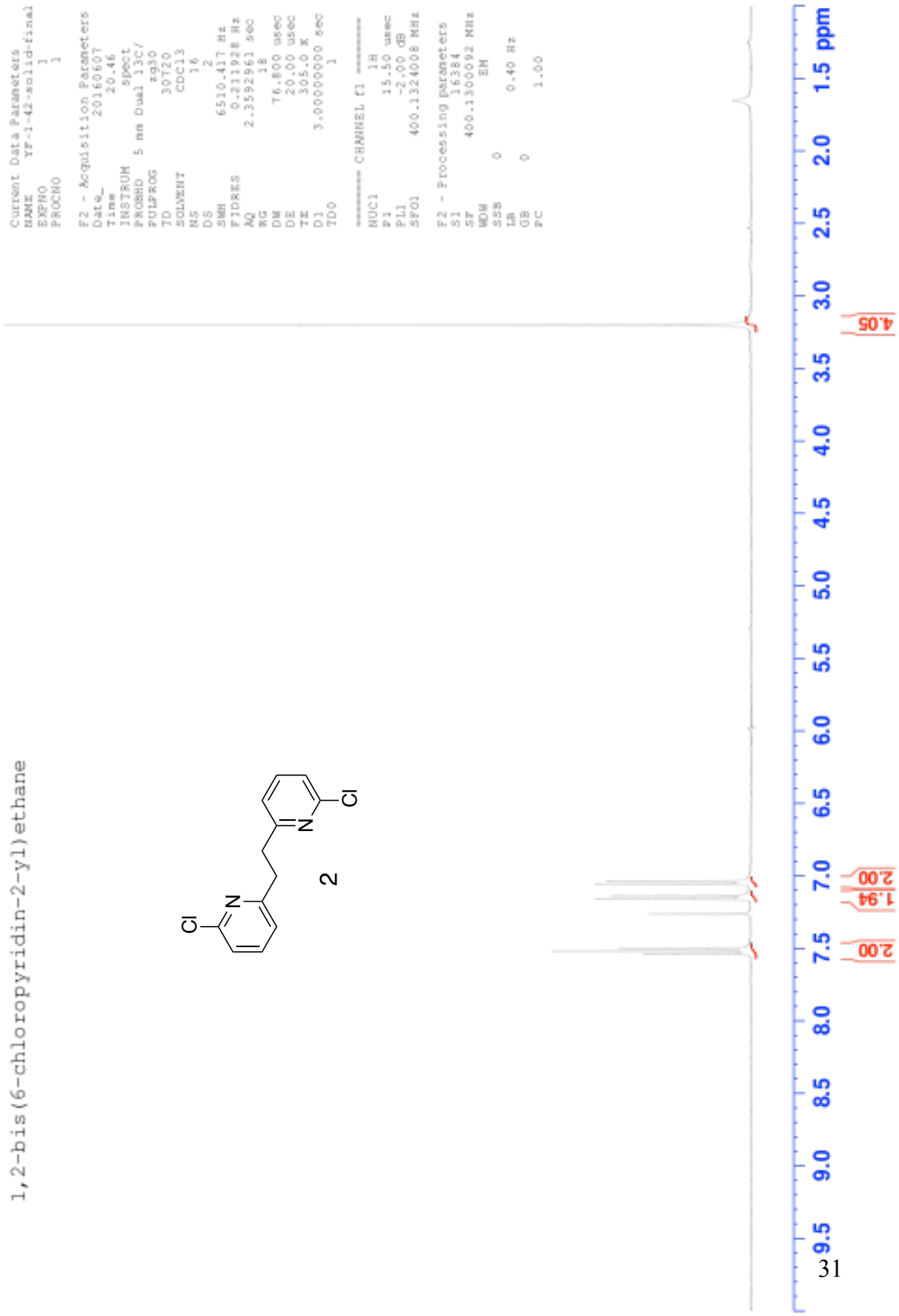
1,2-bis(6-chloropyridin-2-yl)ethane
Current Data Parameters
NAME YF-1-42-solid-final
EXPNO 1
PROCNO 1
F2 - Acquisition Parameters
Date_ 20160607
Time 20.46
INSTRUM spect
PROBHD 5 mm Dual 13C/
PULPROG zg30
TD 30720
SOLVENT CDCl3
NS 16
DS 2
SWH 6510.417 Hz
FIDRES 0.211928 Hz
AQ 2.3592961 sec
RG 18
DW 76.800 usec
DE 20.00 usec
TE 305.0 K
D1 3.00000000 sec
TD0 1
======== CHANNEL f1 ========
NUC1 1H
P1 15.50 usec
PL1 -2.00 dB
SFO1 400.1324008 MHz
F2 - Processing parameters
SI 16384
SF 400.1300092 MHz
WDW EM
SSB 0
LB 0.40 Hz
GB 0
PC 1.00
Cl
N
N
Cl
2
4.05
2.00
1.94
2.00
9.5
9.0
8.5
8.0
7.5
7.0
6.5
6.0
5.5
5.0
4.5
4.0
3.5
3.0
2.5
2.0
1.5 ppm

1,2-bis(6-hydroxypyridin-2-yl)ethane bis(hydrogen chloride)

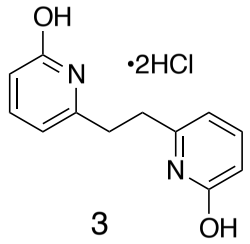

3

```
Current Data Parameters
NAME          YF-1-40-1
EXPNO                 1
PROCNO                1

F2 - Acquisition Parameters
Date_          20160531
Time              10.45
INSTRUM           spect
PROBHD   5 mm Dual 13C/
PULPROG           zg30
TD               30720
SOLVENT           MeOD
NS                   16
DS                    2
SWH           6510.417 Hz
FIDRES        0.211928 Hz
AQ            2.3592961 sec
RG                812.7
DW               76.800 usec
DE               20.00 usec
TE               305.0 K
D1           3.00000000 sec
TD0                   1

======== CHANNEL f1 ========
NUC1                  1H
P1                15.50 usec
PL1               -2.00 dB
SFO1        400.1324008 MHz

F2 - Processing parameters
SI                16384
SF          400.1300072 MHz
WDW                  EM
SSB      0
LB               0.40 Hz
GB       0
PC               1.00
```

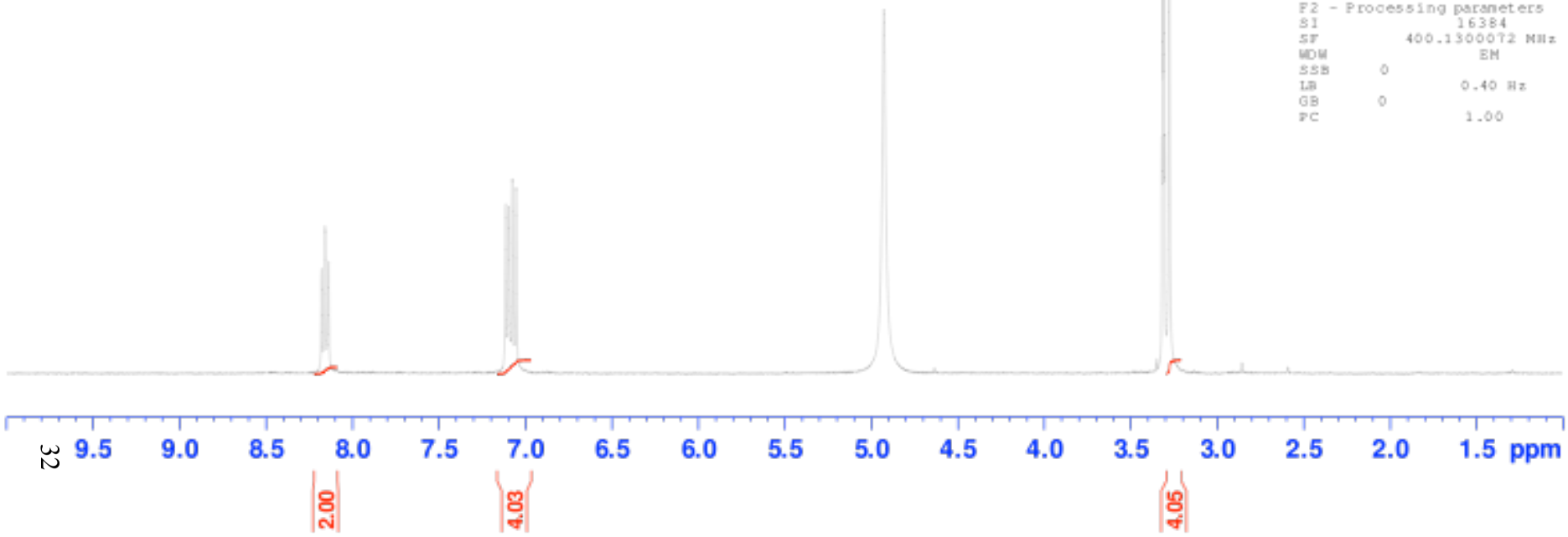

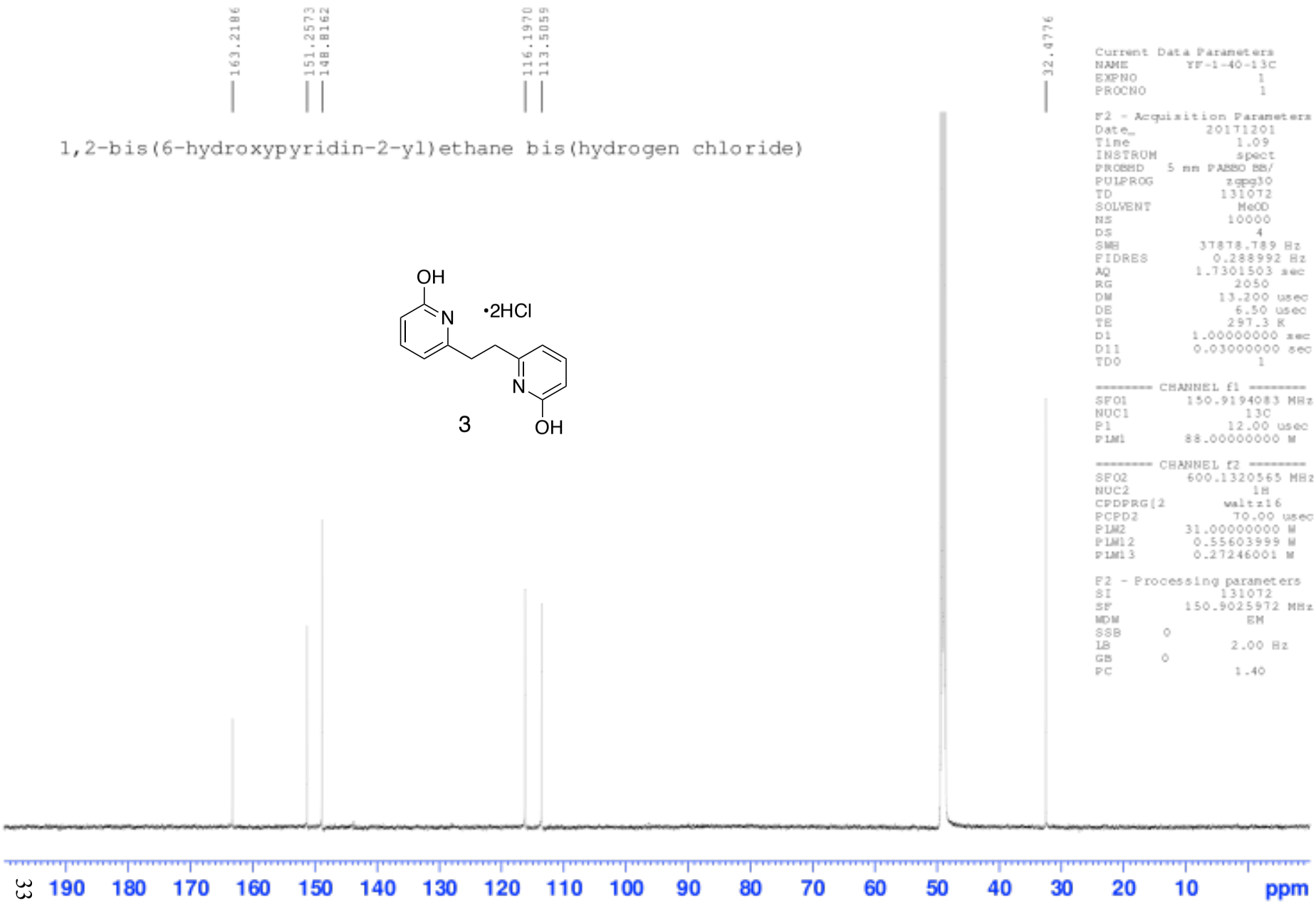
163.2186
151.2573
148.8162
116.1970
113.5059
32.4776
1,2-bis(6-hydroxypyridin-2-yl)ethane bis(hydrogen chloride)
OH
N
•2HCl
N
OH
3
Current Data Parameters
NAME YF-1-40-13C
EXPNO 1
PROCNO 1
F2 - Acquisition Parameters
Date_ 20171201
Time 1.09
INSTRUM spect
PROBHD 5 mm PABBO BB/
PULPROG zgpg30
TD 131072
SOLVENT MeOD
NS 10000
DS 4
SWH 37878.789 Hz
FIDRES 0.288992 Hz
AQ 1.7301503 sec
RG 2050
DW 13.200 usec
DE 6.50 usec
TE 297.3 K
D1 1.00000000 sec
D11 0.03000000 sec
TD0 1
======== CHANNEL f1 ========
SFO1 150.9194083 MHz
NUC1 13C
P1 12.00 usec
PLW1 88.00000000 W
======== CHANNEL f2 ========
SFO2 600.1320565 MHz
NUC2 1H
CPDPRG[2 waltz16
PCPD2 70.00 usec
PLW2 31.00000000 W
PLW12 0.55603999 W
PLW13 0.27246001 W
F2 - Processing parameters
SI 131072
SF 150.9025972 MHz
WDW EM
SSB 0
LB 2.00 Hz
GB 0
PC 1.40
33
190 180 170 160 150 140 130 120 110 100 90 80 70 60 50 40 30 20 10 ppm

Lithium 6,6'-(ethane-1,2-diyl)bis(pyridin-2-olate)

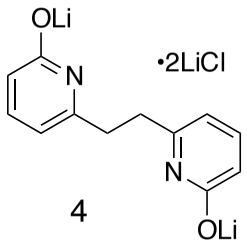

4

Current Data Parameters
NAME YF-1-88-20160908-1
EXPNO 1
PROCNO 1

F2 - Acquisition Parameters
Date_ 20160908
Time 15.37
INSTRUM spect
PROBHD 5 mm Dual 13C/
PULPROG zg30
TD 30720
SOLVENT MeOD
NS 16
DS 2
SWH 4807.692 Hz
FIDRES 0.156500 Hz
AQ 3.1948800 sec
RG 406.4
DW 104.000 usec
DE 20.00 usec
TE 305.0 K
D1 3.00000000 sec
TD0 1

======== CHANNEL f1 ========
NUC1 1H
P1 15.50 usec
PL1 -2.00 dB
SFO1 400.1320007 MHz

F2 - Processing parameters
SI 16384
SF 400.1300074 MHz
WDW EM
SSB 0
LB 0.40 Hz
GB 0
PC 1.00

[2.1.1]-(2,6)-9,16-dioxapyridinophane (O2-L)

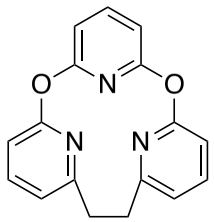

O_2-L

```
Current Data Parameters
NAME      YF-1-95-FinalProdox
EXPNO                    1
PROCNO                   1

F2 - Acquisition Parameters
Date_          20161003
Time               19.48
INSTRUM            spect
PROBHD   5 mm BBI 1H/19
PULPROG            zg30
TD                48074
SOLVENT           CDCl3
NS                   32
DS                    2
SWH           7211.539 Hz
FIDRES         0.150009 Hz
AQ            3.3331306 sec
RG                  203
DW               69.333 usec
DE               10.00 usec
TE               298.0 K
D1            2.50000000 sec
TD0                  1

======== CHANNEL f1 ========
SFO1        600.1330006 MHz
NUC1               1H
P1                9.70 usec
PLW1        10.39999962 W

F2 - Processing parameters
SI                65536
SF          600.1300092 MHz
WDW                EM
SSB      0
LB              0.20 Hz
GB       0
PC                3.00
```

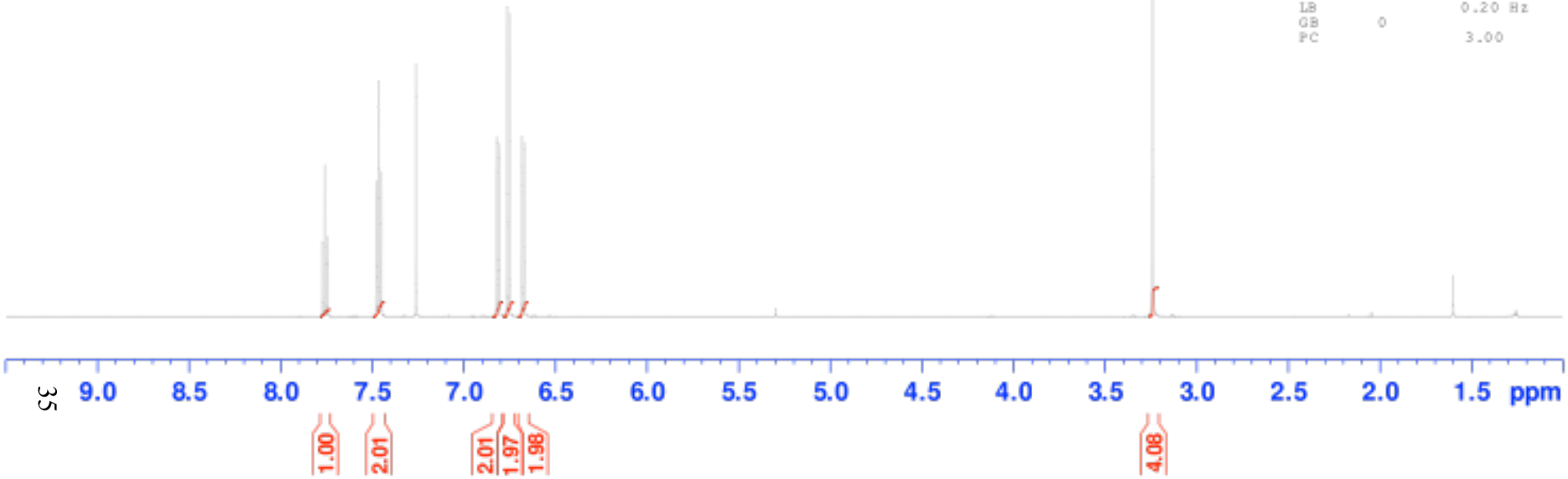

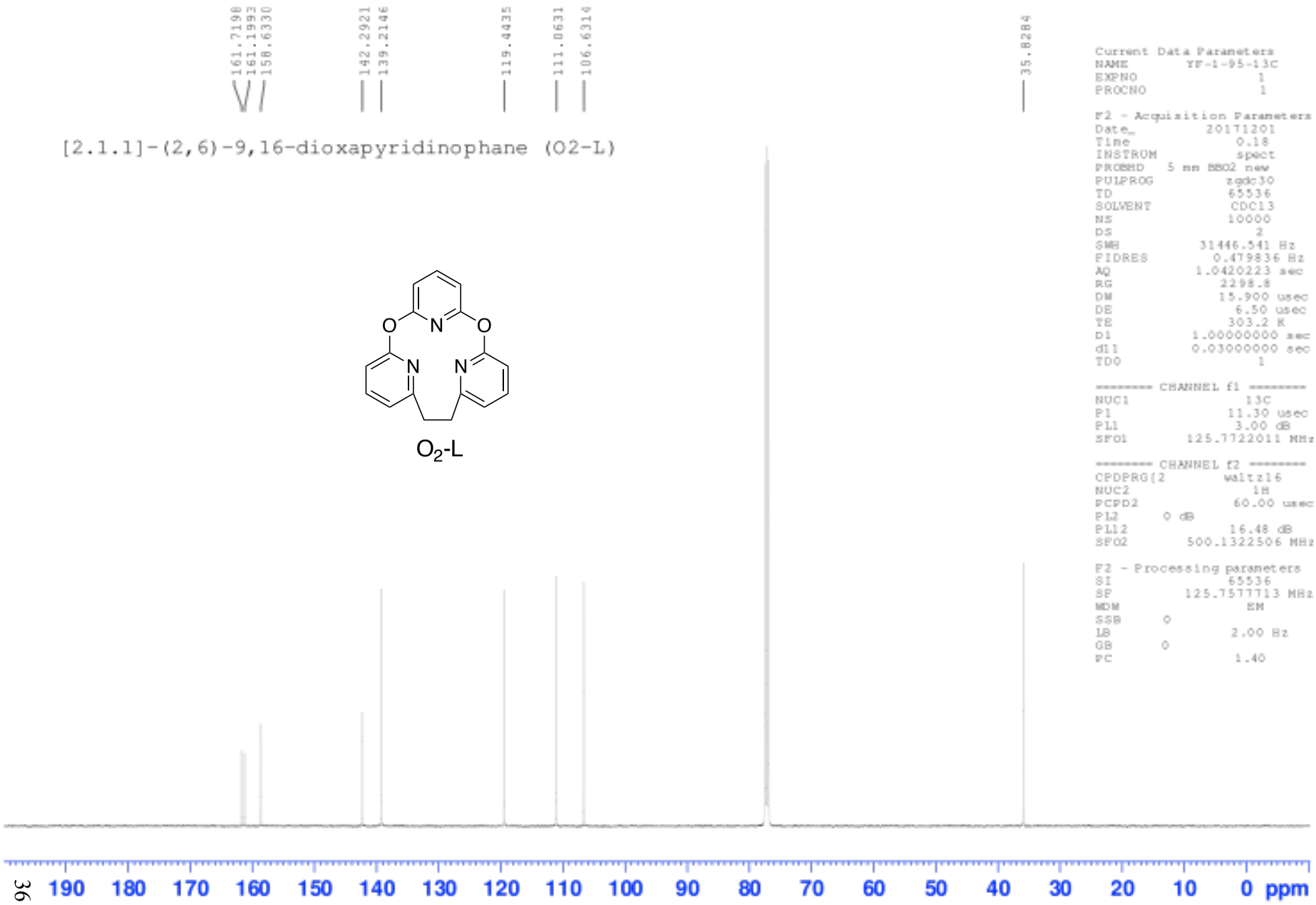
161.7196
161.1993
158.6330
142.2921
139.2146
119.4435
111.0631
106.6310
35.8284
[2.1.1]-(2,6)-9,16-dioxapyridinophane (O2-L)
O
N
O
N
N
O2-L
Current Data Parameters
NAME YF-1-95-13C
EXPNO 1
PROCNO 1
F2 - Acquisition Parameters
Date_ 20171201
Time 0.18
INSTRUM spect
PROBHD 5 mm BBO2 new
PULPROG zgdc30
TD 65536
SOLVENT CDCl3
NS 10000
DS 2
SWH 31446.541 Hz
FIDRES 0.479836 Hz
AQ 1.0420223 sec
RG 2298.8
DW 15.900 usec
DE 6.50 usec
TE 303.2 K
D1 1.00000000 sec
d11 0.03000000 sec
TD0 1
======== CHANNEL f1 ========
NUC1 13C
P1 11.30 usec
PL1 3.00 dB
SFO1 125.7722011 MHz
======== CHANNEL f2 ========
CPDPRG[2 waltz16
NUC2 1H
PCPD2 60.00 usec
PL2 0 dB
PL12 16.48 dB
SFO2 500.1322506 MHz
F2 - Processing parameters
SI 65536
SF 125.7577713 MHz
WDW EM
SSB 0
LB 2.00 Hz
GB 0
PC 1.40
190 180 170 160 150 140 130 120 110 100 90 80 70 60 50 40 30 20 10 0 ppm

(O2-L)PdCl2

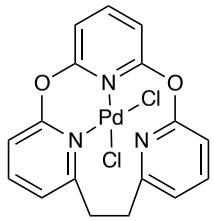


```
Current Data Parameters
NAME            YF-1-101
EXPNO                  1
PROCNO                 1

F2 - Acquisition Parameters
Date_           20161013
Time              12.06
INSTRUM            spect
PROBHD   5 mm Dual 13C/
PULPROG            zg30
TD                30720
SOLVENT           CD2Cl2
NS                   32
DS                    2
SWH             6510.417 Hz
FIDRES          0.211928 Hz
AQ             2.3592961 sec
RG                   18
DW               76.800 usec
DE               20.00 usec
TE                305.0 K
D1            3.00000000 sec
TD0                    1

======== CHANNEL f1 ========
NUC1                  1H
P1                15.50 usec
PL1               -2.00 dB
SFO1         400.1324008 MHz

F2 - Processing parameters
SI                 16384
SF           400.1300000 MHz
WDW                   EM
SSB      0
LB                0.40 Hz
GB       0
PC                1.00
```

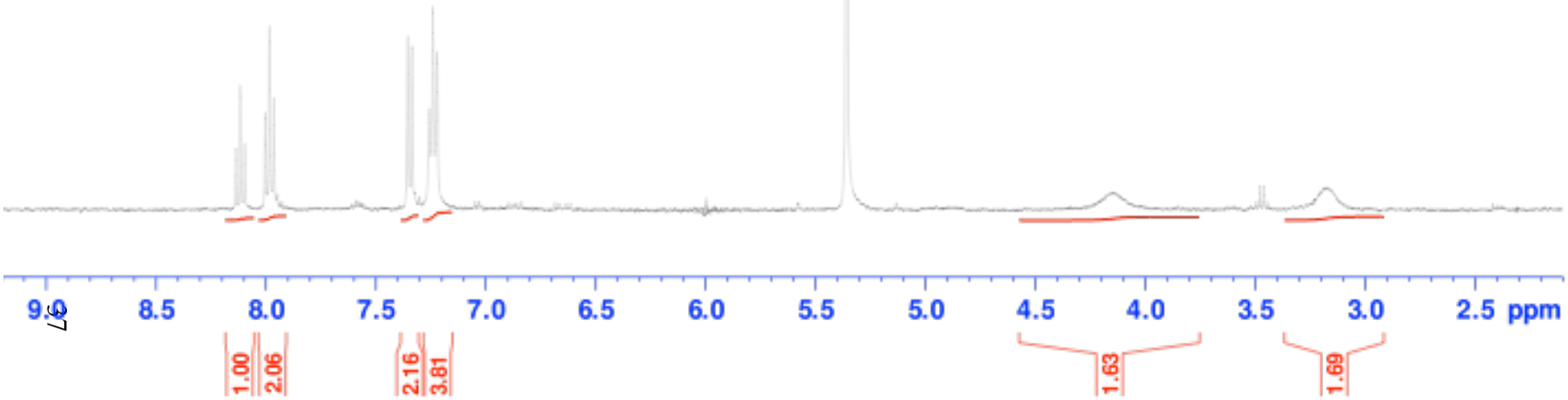

(O2-L)PdCl2

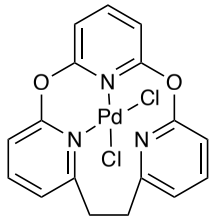


```
Current Data Parameters
NAME                  VT-1
EXPNO                    2
PROCNO                   1

F2 - Acquisition Parameters
Date_              20161027
Time                 16.29
INSTRUM              spect
PROBHD    5 mm BBO2 new
PULPROG               zg30
TD                   49152
SOLVENT             CD2Cl2
NS                      894
DS                        0
SWH                8012.820 Hz
FIDRES            0.163021 Hz
AQ                3.0670848 sec
RG                   574.7
DW                  62.400 use
DE                   6.50 use
TE                  220.2 K
D1                2.00000000 se
TD0                       1

======== CHANNEL f1 ======
NUC1                     1H
P1                   10.75 use
PL1        0 dB
SFO1          500.1330880 MH

F2 - Processing parameters
SI                    32768
SF              500.1300212 MH
WDW                     EM
SSB        0
LB                   0.30 Hz
GB         0
PC                   1.00
```

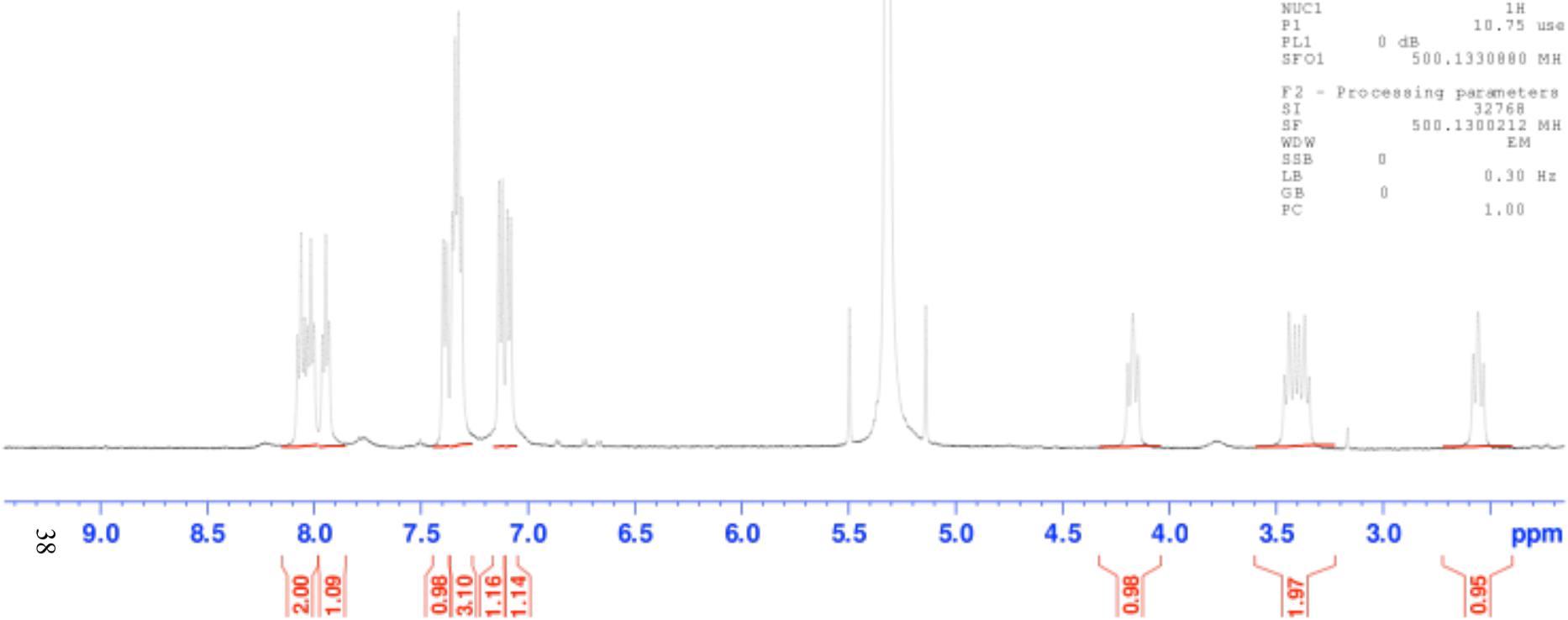

(O2-L)CuCl

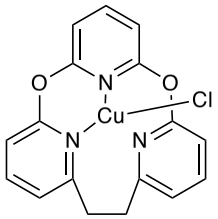

fluxional

```
Current Data Parameters
NAME            YF-1-111
EXPNO                  1
PROCNO                 1

F2 - Acquisition Parameters
Date_           20161107
Time               10.49
INSTRUM            spect
PROBHD   5 mm Dual 13C/
PULPROG            zg30
TD                30720
SOLVENT          CD2Cl2
NS                    16
DS                     2
SWH            6510.417 Hz
FIDRES        0.211928 Hz
AQ            2.3592961 sec
RG                    18
DW               76.800 usec
DE               20.00 usec
TE                305.0 K
D1            3.00000000 sec
TD0                    1

======== CHANNEL f1 ========
NUC1                  1H
P1                15.50 usec
PL1               -2.00 dB
SFO1         400.1324008 MHz

F2 - Processing parameters
SI                 16384
SF           400.1300000 MHz
WDW                   EM
SSB      0
LB                0.40 Hz
GB       0
PC                1.00
```

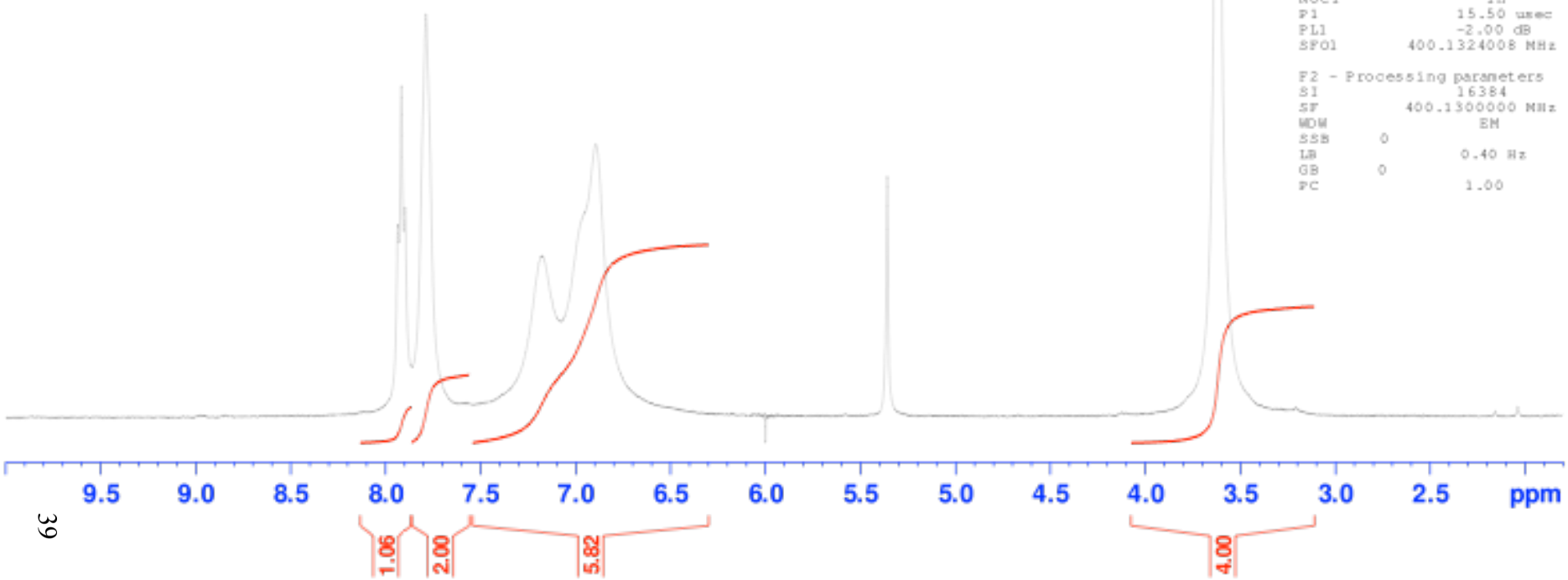

References

(1) Garnett, J. L.; Hodges, R. J. Homogeneous Metal-Catalyzed Exchange of Aromatic Compounds. A New General Isotopic Hydrogen Labeling Procedure. *J. Am. Chem. Soc.* **1967,** *89* (17), 4546.

(2) Goldshleger, N. F.; Shteinman, A. A.; Shilov, A. E.; Eskova, V. V. Alkane Reactions in Solutions of Chloride Complexes of Platinum. *Zhurnal Fizicheskoi Khimii* **1972,** *46* (5), 1353.

(3) Labinger, J. A. Platinum-Catalyzed C-H Functionalization. *Chem. Rev.* **2017,** *117* (13), 8483.

(4) Lersch, M.; Tilset, M. Mechanistic Aspects of C-H Activation by Pt Complexes. *Chem. Rev.* **2005,** *105* (6), 2471.

(5) Lincoln, S. F.; Merbach, A. E.; Sykes, A. G. In *Advances in Inorganic Chemistry*; Academic Press, 1995; Vol. 42.

(6) Langford, C. H.; Gray, H. B. *Ligand Substitution Processes*; Benjamin: New York, 1965.

(7) Basolo, F.; Pearson, R. G. *Mechanisms of Inorganic Reactions*; John Wiley and Sons: New York, 1967.

(8) Atwood, J. D. *Inorganic and Organometallic Reaction Mechanisms*; VCH: New York, 1997.

(9) Vedernikov, A. N.; Pink, M.; Caulton, K. G. Design and Synthesis of Tridentate Facially Chelating Ligands of the [2.n.1]-(2,6)-Pyridinophane Family. *J. Org. Chem.* **2003,** *68* (12), 4806.

(10) Vedernikov, A. N.; Caulton, K. G. Control of H-C(sp^3) Bond Cleavage Stoichiometry: Clean Reversible Alkyl Ligand Exchange with Alkane in $[LPt(Alk)(H)_2]^+$ (L = [2.1.1]-(2,6)-Pyridinophane). *Angew. Chem. Int. Ed.* **2002,** *41* (21), 4102.

(11) Vedernikov, A. N.; Huffman, J. C.; Caulton, K. G. [2.1.1]-(2,6)-Pyridinophane(L)-controlled Alkane C-H Bond Cleavage: $(L)PtMe_2H^+$ As a Precursor to the Geometrically "tense" Transient $(L)PtMe^+$. *New J. Chem.* **2003,** *27* (4), 665.

(12) Vedernikov, A. N.; Caulton, K. G. N-Pt-IV-H/N-H...Pt-II Intramolecular Redox Equilibrium In a Product of H-C(sp2) Cleavage and Unusual Alkane/arene C-H Bond Selectivity of ([2.1.1]-Pyridinophane)$Pt^{II}(CH_3)$. *ChemComm* **2003,** (3), 358.

(13) Vedernikov, A. N.; Huffman, J. C.; Caulton, K. G. [n.1.1]-(2,6)-pyridinophanes: A new ligand type imposing unusual metal coordination geometries. *Inorg. Chem.* **2002,** *41* (25), 6867.

(14) Florio, S.; Luisi, R. Aziridinyl Anions: Generation, Reactivity, and Use in Modern Synthetic Chemistry. *Chem. Rev.* **2010,** *110* (9), 5128.

(15) Hu, X. E. Nucleophilic Ring Opening of Aziridines. *Tetrahedron* **2004,** *60* (12), 2701.

(16) Pellissier, H. Recent Developments in Asymmetric Aziridination. *Tetrahedron* **2010,** *66* (8), 1509.

(17) Pellissier, H. Recent Developments in Asymmetric Aziridination. *Adv. Synth. Catal.* **2014,** *356* (9), 1899.

(18) Singh, G. S.; D'Hooghe, M.; De Kimpe, N. Synthesis and Reactivity of C-Heteroatom-Substituted Aziridines. *Chem. Rev.* **2007,** *107* (5), 2080.

(19) Ohno, H. Synthesis and Applications of Vinylaziridines and Ethynylaziridines. *Chem. Rev.* **2014,** *114* (16), 7784.

(20) Bencivenni, G.; Righi, P.; Lunazzi, L.; Ranieri, S.; Mancinelli, M.; Mazzanti, A. Enantioselective Preparation, Conformational Analysis and Absolute Configuration of Highly Substituted Aziridines. *Chirality* **2015,** *27* (12), 875.

(21) Lai, B. N.; Qiu, J. F.; Zhang, H. X.; Nie, J.; Ma, J. A. Stereoselective Synthesis of Fused Aziridines via One-Pot Sequential Decarboxylative Mannich Reaction and Oxidative C-H Amination of Cyclic Imines with beta-Ketoacids. *Org. Lett.* **2016,** *18* (3), 520.

(22) Chang, J. W. W.; Ton, T. M. U.; Chan, P. W. H. Transition-metal-catalyzed Aminations and Aziridinations of C-H and C=C Bonds with Iminoiodinanes. *Chem. Rec.* **2011,** *11* (6), 331.

(23) Minakata, S. Utilization of N-X Bonds in The Synthesis of N-Heterocycles. *Acc. Chem. Res.* **2009,** *42* (8), 1172.

(24) Intrieri, D.; Zardi, P.; Caselli, A.; Gallo, E. Organic Azides: "Energetic Reagents" for The Intermolecular Amination of C-H Bonds. *ChemComm* **2014,** *50* (78), 11440.

(25) Uchida, T.; Katsuki, T. Asymmetric Nitrene Transfer Reactions: Sulfimidation, Aziridination and C-H Amination Using Azide Compounds as Nitrene Precursors. *Chem. Rec.* **2014,** *14* (1), 117.

(26) Damiano, C.; Intrieri, D.; Gallo, E. Aziridination of Alkenes Promoted by Iron or Ruthenium Complexes. *Inorganica Chim. Acta* **2017**.

(27) Ju, M.; Weatherly, C. D.; Guzei, I. A.; Schomaker, J. M. Chemo- and Enantioselective Intramolecular Silver-Catalyzed Aziridinations. *Angew. Chem. Int. Ed.* **2017,** *56* (33), 9944.

(28) Vedernikov, A. N.; Caulton, K. G. Angular Ligand Constraint Yields an Improved Olefin Aziridination Catalyst. *Org. Lett.* **2003,** *5* (15), 2591.

(29) Perez, P. J.; Brookhart, M.; Templeton, J. L., A Copper(I) Catalyst for Carbene and Nitrene Transfer to Form Cyclopropanes, Cyclopropenes, and Aziridines. *Organometallics* **1993,** *12* (2), 261-262.

(30) Langham, C.; Piaggio, P.; Bethell, D.; Lee, D. F.; McMorn, P.; Page, P. C. B.; Willock, D. J.; Sly, C.; Hancock, F. E.; King, F.; Hutchings, G. J., Catalytic Heterogeneous Aziridination of Alkenes Using Microporous Materials. *ChemComm* **1998,** (15), 1601-1602.

(31) Amisial, L. D.; Dai, X. L.; Kinney, R. A.; Krishnaswamy, A.; Warren, T. H., Cu(I) β-Diketiminates for Alkene Aziridination: Reversible Cu-arene Binding and Catalytic Nitrene Transfer from PhI=NTs. *Inorg. Chem.* **2004,** *43* (21), 6537-6539.

(32) Halfen, J. A.; Hallman, J. K.; Schultz, J. A.; Emerson, J. P., Remarkably Efficient Olefin Aziridination Mediated by A New Copper(II) Complex. *Organometallics* **1999,** *18* (26), 5435-5437.

(33) Nakanishi, M.; Salit, A.-F.; Bolm, C., Iron-catalyzed Aziridination Reactions. *Adv. Synth. Catal.* **2008,** *350* (11-12), 1835-1840.

(34) Liu, P.; Wong, E. L.-M.; Yuen, A. W.-H.; Che, C.-M., Highly Efficient Alkene Epoxidation and Aziridination Catalyzed by Iron(II) Salt + 4,4',4''-trichloro-2,2': 6',2''-terpyridine/4,4''-dichloro-4'-O-PEG-OCH3-2,2': 6',2''-terpyridine. *Org. Lett.* **2008,** *10* (15), 3275-3278.

(35) Heuss, B. D.; Mayer, M. F.; Dennis, S.; Hossain, M. M., Iron Mediated Nitrenoid Transfer: $(\eta^5\text{-}C_5H_5)Fe(CO)_2(THF)^+ BF_4^-$ Catalyzed Aziridination of Olefins. *Inorganica Chim. Acta* **2003,** *342*, 301-304.

(36) Ponduru, T. T.; Dias, H. V. R., Dinuclear Zinc(II) Pyrazolates With Different Degrees of Ring-Fluorination and Their Use in Zinc(II) Mediated Olefin Aziridination. *Dalton Trans.* **2017,** *46* (43), 14733-14737.

(37) Cui, Y.; He, C., Efficient Aziridination of Olefins Catalyzed by a Unique Disilver(I) Compound. *J. Am. Chem. Soc.* **2003,** *125* (52), 16202-16203.

(38) Zhang, J. L.; Huang, J. S.; Che, C. M., Oxidation Chemistry of Poly(ethylene glycol)-Supported Carbonylruthenium(II) and Dioxoruthenium(VI) meso-Tetrakis(pentafluorophenyl)porphyrin. *Chem. Eur. J.* **2006,** *12* (11), 3020-3031.